05-10 May 2010

# TECH BRIEFS

NATIONAL AERONAUTICS AND SPACE ADMINISTRATION

# INTRODUCTION

Tech Briefs are short announcements of innovations originating from research and development activities of the National Aeronautics and Space Administration. They emphasize information considered likely to be transferable across industrial, regional, or disciplinary lines and are issued to encourage commercial application.

## Availability of NASA Tech Briefs and TSPs

Requests for individual Tech Briefs or for Technical Support Packages (TSPs) announced herein should be addressed to

**National Technology Transfer Center**
Telephone No. **(800) 678-6882** or via World Wide Web at **www.nttc.edu**

Please reference the control numbers appearing at the end of each Tech Brief. Information on NASA's Innovative Partnerships Program (IPP), its documents, and services is also available at the same facility or on the World Wide Web at **http:/ / www.nasa.gov/ offices/ ipp/ network/ index.html**

Innovative Partnerships Offices are located at NASA field centers to provide technology-transfer access to industrial users. Inquiries can be made by contacting NASA field centers listed below.

## NASA Field Centers and Program Offices

**Ames Research Center**
Lisa L. Lockyer
(650) 604-1754
lisa.l.lockyer@nasa.gov

**Dryden Flight Research Center**
Yvonne D. Gibbs
(661) 276-3720
yvonne.d.gibbs@nasa.gov

**Glenn Research Center**
Kathy Needham
(216) 433-2802
kathleen.k.needham@nasa.gov

**Goddard Space Flight Center**
Nona Cheeks
(301) 286-5810
nona.k.cheeks@nasa.gov

**Jet Propulsion Laboratory**
Andrew Gray
(818) 354-3821
gray@jpl.nasa.gov

**Johnson Space Center**
information
(281) 483-3809
jsc.techtran@mail.nasa.gov

**Kennedy Space Center**
David R. Makufka
(321) 867-6227
david.r.makufka@nasa.gov

**Langley Research Center**
Elizabeth B. Plentovich
(757) 864-2857
elizabeth.b.plentovich@nasa.gov

**Marshall Space Flight Center**
Jim Dowdy
(256) 544-7604
jim.dowdy@msfc.nasa.gov

**Stennis Space Center**
Ramona Travis
(228) 688-3832
ramona.e.travis@nasa.gov

**Carl Ray, Program Executive**
Small Business Innovation Research (SBIR) & Small Business Technology Transfer (STTR) Programs
(202) 358-4652
carl.g.ray@nasa.gov

**Doug Comstock, Director**
Innovative Partnerships Program Office
(202) 358-2221
doug.comstock@nasa.gov

# TECH BRIEFS

## NATIONAL AERONAUTICS AND SPACE ADMINISTRATION



This document was prepared under the sponsorship of the National Aeronautics and Space Administration. Neither the United States Government nor any person acting on behalf of the United States Government assumes any liability resulting from the use of the information contained in this document, or warrants that such use will be free from privately owned rights.

## Instrument for Analysis of Greenland's Glacier Mills

*NASA's Jet Propulsion Laboratory, Pasadena, California*

A new instrument is used to study the inner workings of Greenland's glacier mills by riding the currents inside a glacier's moulin. The West Greenland Moulin Explorer instrument was deployed into a tubular shaft to autonomously record temperature, pressure, 3D acceleration, and location. It is built with a slightly positive buoyancy in order to assist in recovery.

The unit is made up of several components. A 3-axis MEMS (microelectromechanical systems) accelerometer with 0.001-g resolution forms the base of the unit. A pressure transducer is added that is capable of withstanding 500 psi (≈3.4 MPa), and surviving down to –40 °C. An Iridium modem sends out data every 10 minutes. The location is traced by a GPS (Global Positioning System) unit. This GPS unit is also used for recovery after the mission. Power is provided by a high-capacity lithium thionyl chloride D-sized battery. The accelerometer is housed inside a cylindrical, foot-long (≈30 cm) polyvinyl chloride (PVC) shell sealed at each end with acrylic. The pressure transducer is attached to one of these lids and a MEMS accelerometer to the other, recording 100 samples per second per axis.

*This work was done by Alberto E. Behar, Jaret B. Matthews, and Hung B. Tran of the Jet Propulsion Laboratory; Konrad Steffen, Dan McGrath, and Thomas Phillips of the University of Colorado Boulder; and summer students Andrew Elliot, Sean O'Hern, Colin Lutz, Sujita Martin, and Henry Wang for NASA's Jet Propulsion Laboratory. Further information is contained in a TSP (see page 1).* NPO-46514

## Cryogenic Moisture Apparatus

**Testing for moisture uptake in materials can be performed under standardized cryogenic conditions.**

*John F. Kennedy Space Center, Florida*

The Cryogenic Moisture Apparatus (CMA) is designed for quantifying the amount of moisture from the surrounding air that is taken up by cryogenic-tank-insulating material specimens while under typical conditions of use. More specifically, the CMA holds one face of the specimen at a desired low temperature (e.g., the typical liquid-nitrogen temperature of 77 K) while the opposite face remains exposed to humid air at ambient or near-ambient temperature. The specimen is weighed before and after exposure in the CMA. The difference between the "after" and "before" weights is determined to be the weight of moisture absorbed by the specimen.

Notwithstanding the term "cryogenic," the CMA is not limited to cryogenic applications: the low test temperature can be any temperature below ambient, and the specimen can be made of any material affected by moisture in air. The CMA is especially well suited for testing a variety of foam insulating materials, including those on the space-shuttle external cryogenic tanks, on other cryogenic vessels, and in refrigerators used for transporting foods, medicines, and other perishables. Testing is important because absorbed moisture not only adds weight but also, in combina-

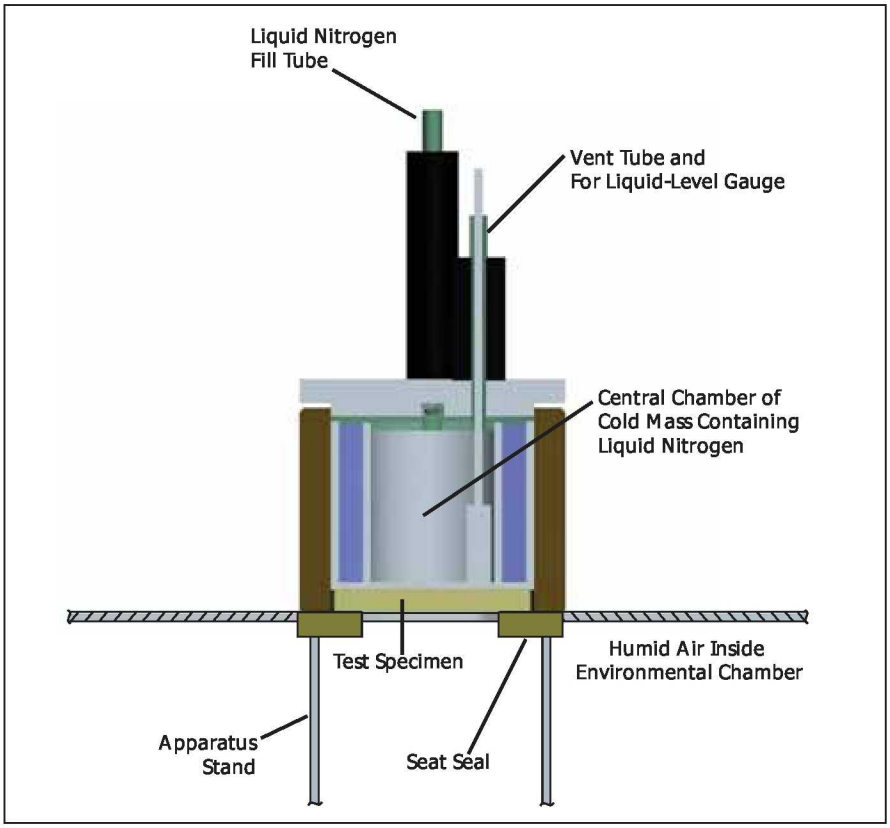


The **Cryogenic Moisture Apparatus** imposes a low temperature on a central portion of the upper face of the specimen while the bottom face of the specimen is exposed to moist air at ambient or near-ambient temperature. This is a simplified view.

tion with thermal cycling, can contribute to damage that degrades insulating performance. Materials are changed internally when subjected to large sub-ambient temperature gradients.

The CMA (see figure) includes a cold mass in the form of an insulated vessel filled with liquid nitrogen or other suitable liquid at a desired below-ambient temperature. The 200-mm diameter specimen is placed over an opening on the top of an environmental chamber, wherein a temperature of 293 K and relative humidity of 90 percent are maintained in still air at ambient atmospheric pressure. The cold mass is placed atop the specimen, and a 152-mm-diameter cold surface at the bottom of the cold mass makes contact with the top surface of the specimen. The bottom surface of the specimen is exposed to the atmosphere inside the environmental chamber. Temperatures at the top and bottom surfaces of the specimen are measured by thermocouples and are monitored and recorded. The cold mass includes features that guard the outer edge surface of the specimen against substantial heat leakage and against intrusion of moisture so that the uptake of water or ice occurs only or primarily in the vertical, through-the-thickness direction. A typical test run lasts 8 hours from the beginning of cooldown, but test time can be changed as needed to achieve steady-state uptake of moisture.

*This work was done by James Fesmire, Trent Smith, Robert Breakfield, and Kevin Boughner of Kennedy Space Center and Kenneth Heckle and Barry Meneghelli of Sierra Lobo, Inc. Further information is contained in a TSP (see page 1).* ***KSC-13049***

# A Transportable Gravity Gradiometer Based on Atom Interferometry

## Gravity field mapping technology enables more detailed study of dynamic Earth processes like climate change.

*NASA's Jet Propulsion Laboratory, Pasadena, California*

A transportable atom interferometer-based gravity gradiometer has been developed at JPL to carry out measurements of Earth's gravity field at ever finer spatial resolutions, and to facilitate high-resolution monitoring of temporal variations in the gravity field from ground- and flight-based platforms. Existing satellite-based gravity missions such as CHAMP and GRACE measure the gravity field via precise monitoring of the motion of the satellites; i.e. the satellites themselves function as test masses. JPL's quantum gravity gradiometer employs a quantum phase measurement technique, similar to that employed in atomic clocks, made possible by recent advances in laser cooling and manipulation of atoms. This measurement technique is based on atom-wave interferometry, and individual laser-cooled atoms are used as drag-free test masses.

The quantum gravity gradiometer employs two identical atom interferometers as precision accelerometers to measure the difference in gravitational acceleration between two points (Figure 1). By using the same lasers for the manipulation of atoms in both interferometers, the accelerometers have a common reference frame and non-inertial accelerations are effectively rejected as common-mode noise in the differential measurement of the gravity gradient. As a result, the dual atom interferometer-based gravity gradiometer allows gravity measurements on a moving platform,

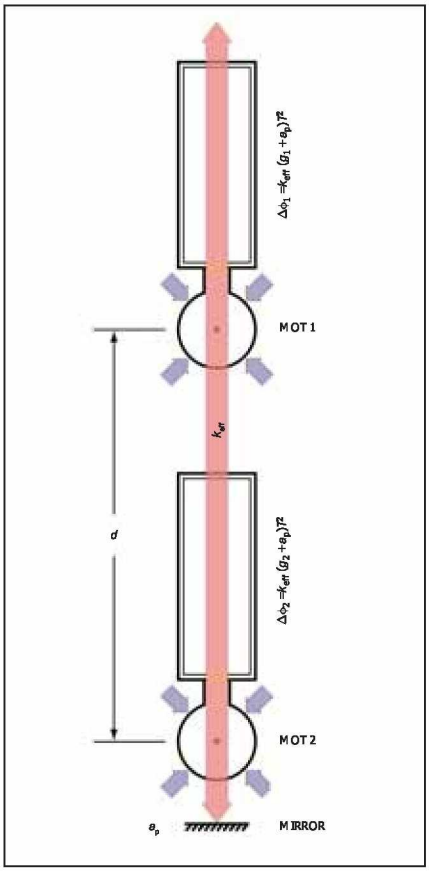


Figure 1. As shown in the schematic of the **Atom Interferometer-Based Gravity Gradiometer,** the dual atom interferometers measure the gravity gradient over the measurement baseline *d*. The platform accelerations $a_p$ are effectively cancelled in the differential measurement. (*T* is the time between pulses, $k_{eff}$ is the effective Raman laser wave number, and *g* is gravitational acceleration.)

Figure 2. The photograph shows the **Quantum Gravity Gradiometer** in the laboratory. The magnetic shields around the lower atom interferometer have been removed for clarity.

while achieving the same long-term stability of the best atomic clocks.

In the laboratory-based prototype (Figure 2), the cesium atoms used in each atom interferometer are initially collected and cooled in two separate magneto-optic traps (MOTs). Each MOT, consisting of three orthogonal pairs of counter-propagating laser beams centered on a quadrupole magnetic field, collects up to $10^9$ atoms. These atoms are then launched vertically as in an "atom fountain" by switching off the magnetic field and introducing a slight frequency shift between pairs of lasers to create a moving rest frame for the trapped atoms. While still in this moving-frame molasses, the laser frequencies are further detuned from the atomic resonance (while maintaining this relative frequency shift) to cool the atom cloud's temperature to 2 μK or below, corresponding to an rms velocity of less than 2 cm/ s. After launch, the cold atoms undergo further state and velocity selection to prepare for atom interferometry. The atom interferometers are then realized using laser-induced stimulated Raman transitions to perform the necessary manipulations of each atom, and the resulting interferometer phase is measured using laser-induced fluorescence for state-normalized detection. More than 20 laser beams with independent controls of frequency, phase, and intensity are required for this measurement sequence.

This instrument can facilitate the study of Earth's gravitational field from surface and air vehicles, as well as from space by allowing gravity mapping from a low-cost, single spacecraft mission. In addition, the operation of atom interferometer-based instruments in space offers greater sensitivity than is possible in terrestrial instruments due to the much longer interrogation times available in the microgravity environment. A space-based quantum gravity gradiometer has the potential to achieve sensitivities similar to the GRACE mission at long spatial wavelengths, and will also have resolution similar to GOCE for measurement at shorter length scales.

*This work was done by Nan Yu, Robert J. Thompson, James R. Kellogg, David C. Aveline, Lute Maleki, and James M. Kohel of Caltech for NASA's Jet Propulsion Laboratory. Further information is contained in a TSP (see page 1).* NPO-46280

# Three Methods of Detection of Hydrazines

## Concentrations could be measured more accurately than in prior methods.

*John F. Kennedy Space Center, Florida*

Three proposed methods for measuring trace quantities of hydrazines involve ionization and detection of hydrazine derivatives. These methods are intended to overcome the limitations of prior hydrazine-detection methods.

Hydrazine (Hz), monomethylhydrazine (MMH), and unsymmetrical dimethylhydrazine (UDMH) are hypergolic fuels and are highly reactive, toxic, and corrosive. A capability to measure concentrations of hydrazines is desirable for detecting leaks and ensuring safety in aerospace settings and in some industrial settings in which these compounds are used. One of the properties (high reactivity) that make it desirable to detect trace amounts of hydrazines also makes it difficult to detect hydrazines and measure their concentrations accurately using prior methods: significant amounts are lost to thermal and catalytic decomposition prior to detection. Further complications arise from the "sticky" nature of hydrazines: Sample hydrazine molecules tend to become irreversibly adsorbed onto solid surfaces with which they come into contact during transport to detectors, giving rise to drift in detector responses.

In each proposed method, the reactive, sticky nature of hydrazines would be turned to advantage by providing a suitably doped substrate surface with which the hydrazines would react. The resulting hydrazine derivatives would be sufficiently less sticky and sufficiently more stable so that fewer molecules would be lost to decomposition or adsorption during transport. Consequently, it would be possible to measure concentration with more sensitivity and less error than in prior techniques.

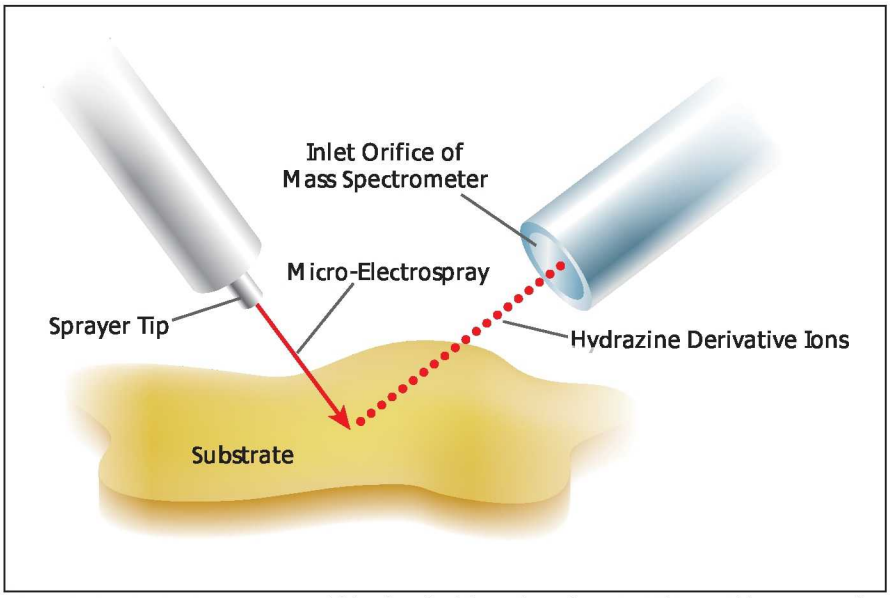


**Hydrazine Derivative Molecules** would be desorbed from the substrate and ionized by a micro-electrospray. The resulting hydrazine derivative ions would be detected by a mass spectrometer.

The first proposed method calls for the use of a recently developed technique known as desorption electrospray ionization (DESI), in which a pneumatically assisted micro-electrospray at ambient pressure is directed at a surface of interest. In this case, the surface of interest would be that of a substrate described above. The impingement of the electrically charged micro-droplets in the spray upon the substrate would dislodge and ionize the hydrazine derivative molecules, giving rise to stable ejected hydrazine derivative

ions, which would then be detected and quantitated by use of a mass spectrometer, ion-mobility spectrometer, or other suitable instrument (see figure).

The second proposed method calls for the use of another recently developed technique known as desorption atmospheric-pressure chemical ionization (DAPCI), in which an atmospheric-pressure corona discharge in the vapor of toluene or another suitable compound is used to generate projectile ions. In this case, the ions would be made to impinge on the substrate, with consequent ejection and ionization of stable hydrazine derivative ions as described above. Again, as described above, the hydrazine derivative ions would be detected and quantitated by use of a mass spectrometer, ion-mobility spectrometer, or other suitable instrument.

In the third proposed method, one would use yet another recently developed desorption-and-ionization technique known as direct analysis in real time (DART). In this technique, a plasma containing excited-state atoms and ions is formed in a gas (e.g., helium or nitrogen) that has a high ionization potential. The excited-state atoms and ions impinge on the surface of a solid sample, causing desorption of low-molecular weight molecules from the sample. In the proposed method, the sample would be the substrate, from which the hydrazine derivative molecules would be desorbed. The desorbed hydrazine derivative molecules would then be ionized and detected as described above.

*This work was done by Timothy Griffin of Kennedy Space Center and Cristina Berger of ASRC Aerospace Corp. Further information is contained in a TSP (see page 1).* ***KSC-13121/2/3***

# Crossed, Small-Deflection Energy Analyzer for Wind/ Temperature Spectrometer

## This analyzer has application in improving the predictability of GPS operations.

*Goddard Space Flight Center, Greenbelt, Maryland*

Determination of neutral winds and ion drifts in low-Earth-orbit missions requires measurements of the angular and energy distributions of the flux of neutrals and ions entering the satellite from the ram direction. The magnitude and direction of the neutral-wind (or ion-drift) determine the location of the maximum in the angular distribution of the flux. Knowledge of the angle of maximum flux with respect to satellite coordinates (pointing) is essential to determine the wind (or ion-drift) vector.

The crossed Small-Deflection Energy Analyzer (SDEA) spectrometer (see Figure 1) occupies minimal volume and consumes minimal power. Designed for upper atmosphere/ ionosphere investigations at Earth altitudes above 100 km, the spectrometer operates by detecting the angular and energy distributions of neutral atoms/ molecules and ions in two mutually perpendicular planes. In this configuration, the two detection planes actually cross at the spectrometer center. It is possible to merge two SDEAs so they share a common optical axis and alternate measurements between two perpendicular planes, and reduce the number of ion sources from two to one. This minimizes the volume and footprint significantly and reduces the ion source power by a factor of two. The area of the entrance aperture affects the number of ions detected/ second and also determines the energy resolution.

Thermionic emitters require heater power of about 100 mW to produce 1 mA of electron beam current. Typically, electron energy is about 100 eV and requires a 100-V supply for electron acceleration to supply an additional 100 mW of power. Thus, ion source power is at most 200 mW. If two ion sources were to be used, the ion source power would be, at most, 400 mW. Detector power, deflection voltage power, and microcontroller and other functions require less than 150 mW. A WTS (wind/ temperature spectrometer) with two separate optical axes would consume about 650 mW, while the crossed SDEA described here consumes about 350 mW.

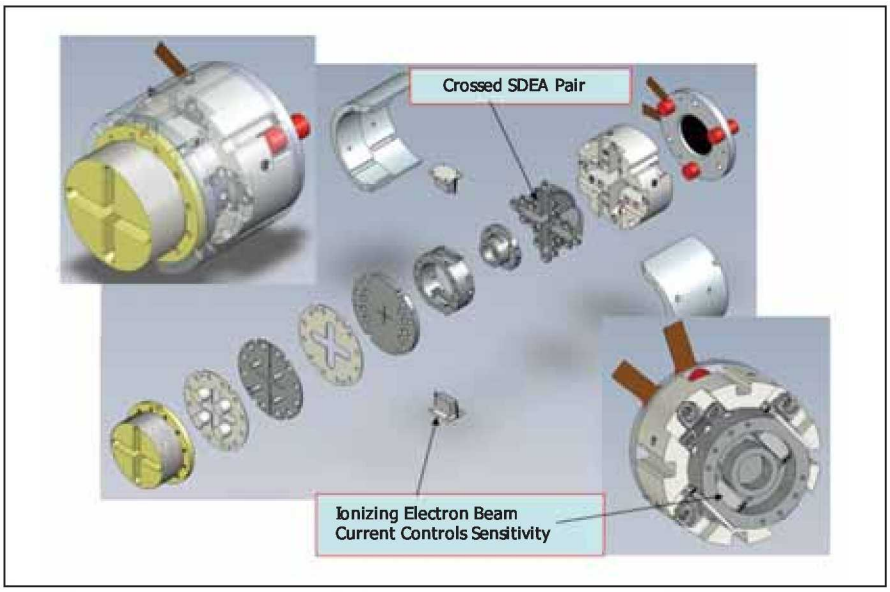


Figure 1. **Drawing of the Crossed SDEA WTS** assembled and in separate parts.

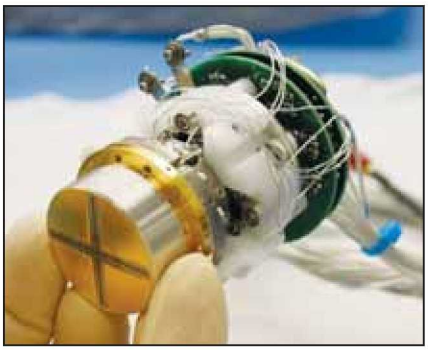

Figure 2. **Photo of the Actual Crossed SDEA WTS** when it was delivered for integration in NRL's ANDE Satellite.

The entrance aperture has a diameter of 0.004 in. (0.10 mm) to provide the required energy resolution between 0.05 and 0.15. This design (see Figure 2) provides a WTS occupying a volume less than 40 $cm^3$, on a footprint of diameter about 1.5 in. (38 mm).

The Crossed SDEA offers many advantages in the measurements of neutral wind and ion drifts in the Earth's thermosphere. As such, it will be useful in future commercial satellites dedicated to monitoring the ionosphere with a view to improving the integrity and predictability of GPS operations.

*This work was done by Federico A. Herrero of Goddard Space Flight Center and Theodore T. Finne of the Naval Research Laboratory. For further information, contact the Goddard Innovative Partnerships Office at (301) 286-5810.*

*This invention is owned by NASA, and a patent application has been filed. Inquiries concerning nonexclusive or exclusive license for its commercial development should be addressed to the Patent Counsel, Goddard Space Flight Center; (301) 286-7351. Refer to GSC-15732-1.*

# Wavefront Correction for Large, Flexible Antenna Reflector

*NASA's Jet Propulsion Laboratory, Pasadena, California*

A wavefront-correction system has been proposed as part of an outer-space radio communication system that would include a large, somewhat flexible main reflector antenna, a smaller subreflector antenna, and a small array feed at the focal plane of these two reflector antennas. Part of the wavefront-correction system would reside in the subreflector, which would be a planar patch-element reflectarray antenna in which the phase shifts of the patch antenna elements would be controlled via microelectromechanical systems (MEMS) radio-frequency (RF) switches. The system would include the following sensing-and-computing subsystems:

- An optical photogrammetric subsystem built around two cameras would estimate geometric distortions of the main reflector;
- A second subsystem would estimate wavefront distortions from amplitudes and phases of signals received by the array feed elements; and
- A third subsystem, built around small probes on the subreflector plane, would estimate wavefront distortions from differences among phases of signals received by the probes.

The distortion estimates from the three subsystems would be processed to generate control signals to be fed to the MEMS RF switches to correct for the distortions, thereby enabling collimation and aiming of the received or transmitted radio beam to the required precision.

*This work was done by William A. Imbriale and Vahraz Jamnejad of Caltech and Yahya Rahmat-Samii, Harish Rajagopalan, and Shenheng Xu of the University of California, Los Angeles, for NASA's Jet Propulsion Laboratory. Further information is contained in a TSP (see page 1).* NPO-46053

# Novel Microstrip-to-Waveguide Feed Employing a Double-Y Junction

**This feed is useful for low-cost measurements involving waveguides up to X-band.**

*NASA's Jet Propulsion Laboratory, Pasadena, California*

Previous microstrip-to-waveguide transitions either required a hermetically sealed waveguide configuration, or a balun that needed to be tuned according to the frequency band of interest. In this design, the balun is realized using a double-Y junction to transition from microstrip to coplanar strip feeding a quasi-Yagi dipole array (see figure). The length of the feed ($L_f$) extending into the waveguide is 15.54 mm. The length of the ground plane below the ULTRALAM substrate is 7.75 mm. The lengths $L_1$, $L_2$, and $L_3$ are 8.50 mm, 4.38 mm, and 2.14 mm, respectively. These lengths were computed via a preliminary optimization aimed at improving the return loss at the band edges.

The waveguide feed was designed to excite the TE10 mode in a WR-90 waveguide, and to operate over the recommended frequencies of 8.2 to 12.4 GHz. The feed employs a Rogers 6010 substrate (dielectric constant $\varepsilon_r \approx 10.2$) bonded with a Rogers ULTRALAM substrate ($\varepsilon_r \approx 2.5$). The ULTRALAM substrate serves to provide mechanical strength for 6010 substrate, and to miti-

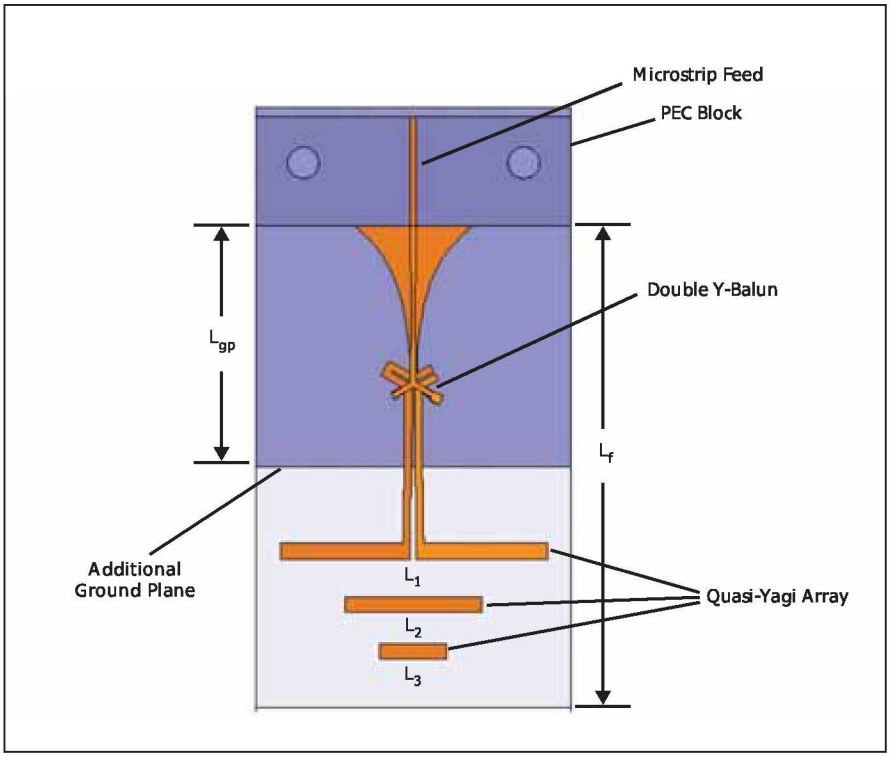


The **Microstrip-to-Waveguide (WR-90) Transition** employing double-Y balun and modeled in HFSS.

gate loses due to parasitic modes (the ground plane is etched on the bottom of this layer due to the topology of the double-Ybalun).

The double-Y balun transitioning from an unbalanced microstrip line to a balanced coplanar strip (CPS) line does not provide inherent impedance transformation; hence, Klopfenstein impedance tapers were synthesized to transition from 50 to 77 Ω in the microstrip section and from 77 to 110 Ω in the CPS section. At the balun junction, the CPS stub lengths were chosen such that the λ/8 resonance is pushed outside the bandwidth of operation. Also, the smallest allowable conductor width and gap spacing were chosen to meet acceptable manufacturing tolerances.

The microstrip-to-waveguide transition has been analyzed numerically using a commercial 3D finite-element electromagnetic solver. The WR-90 waveguide (10.16×22.86×25.56 mm) was modeled as an air box. The 6010 and ULTRALAM substrates were modeled to account for dielectric losses. The microstrip section of the waveguide feed was excited using a 50-Ω lumped port; the output face of the waveguide was modeled as a wave port. The waveguide achieves maximum insertion loss of 0.84 dB, and a minimum insertion loss of 0.32 dB from 8.0 to 12.4 GHz with the ULTRALAM substrate and additional ground. The resulting insertion loss at the band edges is significantly lower. Further improvement in the insertion loss of the waveguide feed can potentially be obtained with continued numerical optimization.

*This work was done by Jaikrishna Venkatesan of Caltech for NASA's Jet Propulsion Laboratory. Further information is contained in a TSP (see page 1).* NPO-42667

# Thin-Film Ferroelectric-Coupled Microstripline Phase Shifters With Reduced Device Hysteresis

**These are useful for electronically steerable ferroelectric reflectarray antennas.**

*John H. Glenn Research Center, Cleveland, Ohio*

This work deals with the performance of coupled microstripline phase shifters (CMPS) fabricated using $Ba_xSr_{1-x}TiO_3$ (BST) ferroelectric thin films. The CMPS were fabricated using commercially available pulsed laser deposition BST films with Ba:Sr ratios of 30:70 and 20:80. Microwave characterization of these CMPS was performed at upper Ku-band frequencies, particularly at frequencies near 16 and 18 GHz. X-ray diffraction studies indicate that the 30:70 films exhibit almost a 1:1 ratio between the in-plane and out-of-plane lattice parameters, suggesting that their cubics create strain-free films suitable for producing CMPS devices with reduced hysteresis in the paraelectric state.

The quality of performance of the CMPS was studied based on their relative phase shift ($\Delta\phi = \phi_{nV} - \phi_{0V}$, where $n$= 0 to 400 volts DC) and insertion loss within the DC bias range of 0 to 400 V (i.e., E-field ranges within 0 to 53 V/μm). The performance of the CMPS was tested as a function of temperature to investigate their operation in the paraelectric, as well as in the ferroelectric, state (i.e., above and below the Curie temperature, respectively). The novel behavior discussed here is based on the experimental observation of the CMPS. Remarkably, these devices were hysteresis-free in the paraelectric state, and only showed Δϕ hysteresis while performing in the ferroelectric state. This behavior, observed for the aforementioned cation ratio, highlights the relevance of good crystalline structure for high-quality CMPS.

Elimination of Δϕ hysteresis is essential for practical microwave applications such as voltage-controlled oscillators and beam-steerable devices, particularly electronically steerable phased array antennas, which require accurate phase shift versus tuning voltage profiles for reliable operation. Accordingly, the optimization of the interplay among film microstructure, Ba content, and dielectric constant is critical for reliable CMPS devices. The origin of hysteresis is most likely related to fixed charges and ferroelectric domain phenomena in the ferroelectric state, as well as remnant ferroelectric domains in the paraelectric state. Consequently, to achieve minimum device hysteresis in the paraelectric domain, the BST films selected for the CMPS devices should be of optimal film composition [i.e., FWHM (full width at half maximum) < 0.05°], with minimum film strain (i.e., in-plane to out-of-plane lattice parameters ratio as close as possible to 1), and moderate values of dielectric constant (≈800 at V= 0) to enable acceptable tunability at manageable insertion losses.

*This work was done by Félix A. Miranda and Robert Romanofsky of Glenn Research Center, Carl H. Mueller of Qinetiq North America, and Frederick Van Keuls of Ohio Aerospace Institute. Further information is contained in a TSP (see page 1).*

*Inquiries concerning rights for the commercial use of this invention should be addressed to NASA Glenn Research Center, Innovative Partnerships Office, Attn: Steve Fedor, Mail Stop 4–8, 21000 Brookpark Road, Cleveland, Ohio 44135. Refer to LEW-18370-1.*

# Two-Stage, 90-GHz, Low-Noise Amplifier

*NASA's Jet Propulsion Laboratory, Pasadena, California*

A device has been developed for coherent detection of the polarization of the cosmic microwave background (CMB). A two-stage amplifier has been designed that covers 75–110 GHz. The device uses the emerging 35-nm InP HEMT technology recently developed at Northrop Grumman Corporation primarily for use at higher frequencies. The amplifier has more than 18 dB gain and less than 35 K noise figure across the band.

These devices have noise less than 30 K at 100 GHz. The development started with design activities at JPL, as well as

characterization of multichip modules using existing InP. Following processing, a test campaign was carried out using single-chip modules at 100 GHz. Successful development of the chips will lead to development of multichip modules, with simultaneous Q and U Stokes parameter detection.

This MMIC (monolithic microwave integrated circuit) amplifier takes advantage of performance improvements intended for higher frequencies, but in this innovation are applied at 90 GHz. The large amount of available gain ultimately leads to lower possible noise performance at 90 GHz.

*This work was done by Lorene A. Samoska, Todd C. Gaier, Stephanie Xenos, Mary M. Soria, Pekka P. Kangaslahti, and Kieran A. Cleary of Caltech; and Linda Ferreira, Richard Lai and Xiaobing Mei of Northrop Grumman Corporation for NASA's Jet Propulsion Laboratory. Further information is contained in a TSP (see page 1).* NPO-46627

# A 311-GHz Fundamental Oscillator Using InP HBT Technology

**This is the first fundamental HBT oscillator operating above 300 GHz.**

*NASA's Jet Propulsion Laboratory, Pasadena, California*

This oscillator uses a single-emitter 0.3-μm InP heterojunction bipolar transistor (HBT) device with maximum frequency of oscillation ($f_{max}$) greater than 500 GHz. Due to high conductor and substrate losses at submillimeter-wave frequencies, a primary challenge is to efficiently use the intrinsic device gain. This was done by using a suitable transmission-line media and circuit topology. The passive components of the oscillator are realized in a two-metal process with benzocyclobutene (BCB) used as the primary transmission line dielectric. The circuit was designed using microstrip transmission lines.

The oscillator is implemented in a common-base topology due to its inherent instability, and the design includes an on-chip resonator, output-matching circuitry, and an injection-locking port, the port being used to demonstrate the injection-locking principle. A free-running frequency of 311.6 GHz has been measured by down-converting the signal. Additionally, injection locking has been successfully demonstrated with up to 17.8 dB of injection-locking gain. The injection-locking reference signal is generated using a 2–20 GHz frequency synthesizer, followed by a doubler, active tripler, a W-band amplifier, and then a passive tripler. Therefore, the source frequency is multiplied 18 times to obtain a signal above 300 GHz that can be used to injection lock the oscillator. Measurement shows that injection locking has improved the phase noise of the oscillator and can be also used for synchronizing a series of oscillators.

A signal conductor is implemented near the BCP-InP interface and the topside of the BCB layer is fully metallized as a signal ground. Because the fields are primarily constrained in the lower permittivity BCB region, this type of transmission line is referred to as an inverted microstrip. In addition, both common-emitter and common-base circuits were investigated to determine optimum topology for oscillator design. The common-base topology required smaller amount of feedback than the common-emitter design, therefore preserving device gain, and was chosen for the oscillator design.

The submillimeter-wave region offers several advantages for sensors and communication systems, such as high resolution and all-weather imaging due to the short-wavelength, and improved communication speeds by access to greater frequency bandwidth. This oscillator circuit is a prototype of the first HBT oscillator operating above 300 GHz. Additional development is necessary to increase the output power of the circuit for radar and imaging applications.

*This work was done by Todd Gaier, King Man Fung, and Lorene Samoska of Caltech and Vesna Radisic, Donald Sawdai, Dennis Scott, and W.R. Deal of Northrop Grumman Corporation for NASA's Jet Propulsion Laboratory. This work was partially supported by the DARPA SWIFT Program and Army Research Laboratory.* ***For more information, download the Technical Support Package (free white paper) at www.techbriefs.com/tsp under the Electronics/Computers category.*** *NPO-44968*

# FPGA Coprocessor Design for an Onboard Multi-angle Spectro-Polarimetric Imager

*NASA's Jet Propulsion Laboratory, Pasadena, California*

A multi-angle spectro-polarimetric imager (MSPI) is an advanced camera system currently under development at JPL for possible future consideration on a satellite-based Aerosol-Cloud-Environment (ACE) interaction study. The light in the optical system is subjected to a complex modulation designed to make the overall system robust against many instrumental artifacts that have plagued such measurements in the past. This scheme involves two photoelastic modulators that are beating in a carefully selected pattern against each other. In order to properly sample this modulation pattern, each of the proposed nine cameras in the system needs to read out its imager array about 1,000 times per second. The onboard processing required to compress this data involves least-squares fits (LSFs) of Bessel functions to data from every pixel in real-time, thus requiring an onboard computing system with advanced data processing capabilities in excess of those commonly available for space flight.

As a potential solution to meet the MSPI onboard processing requirements, an LSF algorithm was developed on the Xilinx Virtex-4FX60 field programmable

gate array (FPGA). In addition to configurable hardware capability, this FPGA includes Power-PC405 microprocessors, which together enable a combination hardware/ software processing system.

A laboratory demonstration was carried out based on a hardware/ software co-designed processing architecture that includes hardware-based data collection and least-squares fitting (computationally), and software-based transcendental function computation (algorithmically complex) on the FPGA. Initial results showed that these calculations can be handled using a combination of the Virtex-4TM Power-PC core and the hardware fabric.

*This work was done by Paula J. Pingree and Thomas A. Werne of Caltech for NASA's Jet Propulsion Laboratory. For more information, contact iaoffice@jpl.nasa.gov. NPO-46614*

# Serrating Nozzle Surfaces for Complete Transfer of Droplets

**Droplets having consistent volumes can be deposited by soft-printing microfluidic devices.**

*Ames Research Center, Moffett Field, California*

A method of ensuring the complete transfer of liquid droplets from nozzles in microfluidic devices to nearby surfaces involves relatively simple geometric modification of the nozzle surfaces. The method is especially applicable to nozzles in print heads and similar devices required to dispense liquid droplets having precise volumes. Examples of such devices include heads for soft printing of ink on paper and heads for depositing droplets of deoxyribonucleic acid (DNA) or protein solutions on glass plates to form microarrays of spots for analysis.

The main purpose served by the present method is to ensure that droplets transferred from a nozzle have consistent volume, as needed to ensure accuracy in microarray analysis or consistent appearance of printed text and images. In soft printing, droplets having consistent volume are generated inside a print head, but in the absence of the present method, the consistency is lost in printing because after each printing action (in which a drop is ejected from a nozzle), a small residual volume of liquid remains attached to the nozzle.

By providing for complete transfer of droplets (and thus eliminating residual liquid attached to the nozzle) the method ensures consistency of volume of transferred droplets. An additional benefit of elimination of residue is prevention of cross-contamination among different liquids printed through the same nozzle — a major consideration in DNA microarray analysis. The method also accelerates the printing process by minimizing the need to clean a printing head to prevent cross-contamination.

Soft printing involves a hydrophobic nozzle surface and a hydrophilic print surface. When the two surfaces are brought into proximity such that a droplet in the nozzle makes contact with the print surface, a substantial portion of the droplet becomes transferred to the print surface. Then as the nozzle and the print surface are pulled apart, the droplet is pulled apart and most of the droplet remains on the print surface. The basic principle of the present method is to reduce the liquid-solid surface energy of the nozzle to a level sufficiently below the intrinsic solid-liquid surface energy of the nozzle material so that the droplet is not pulled apart and, instead, the entire droplet volume becomes transferred to the print surface. In this method, the liquid-solid surface energy is reduced by introducing artificial surface roughness in the form of micromachined serrations on the inner nozzle surface (see figure).

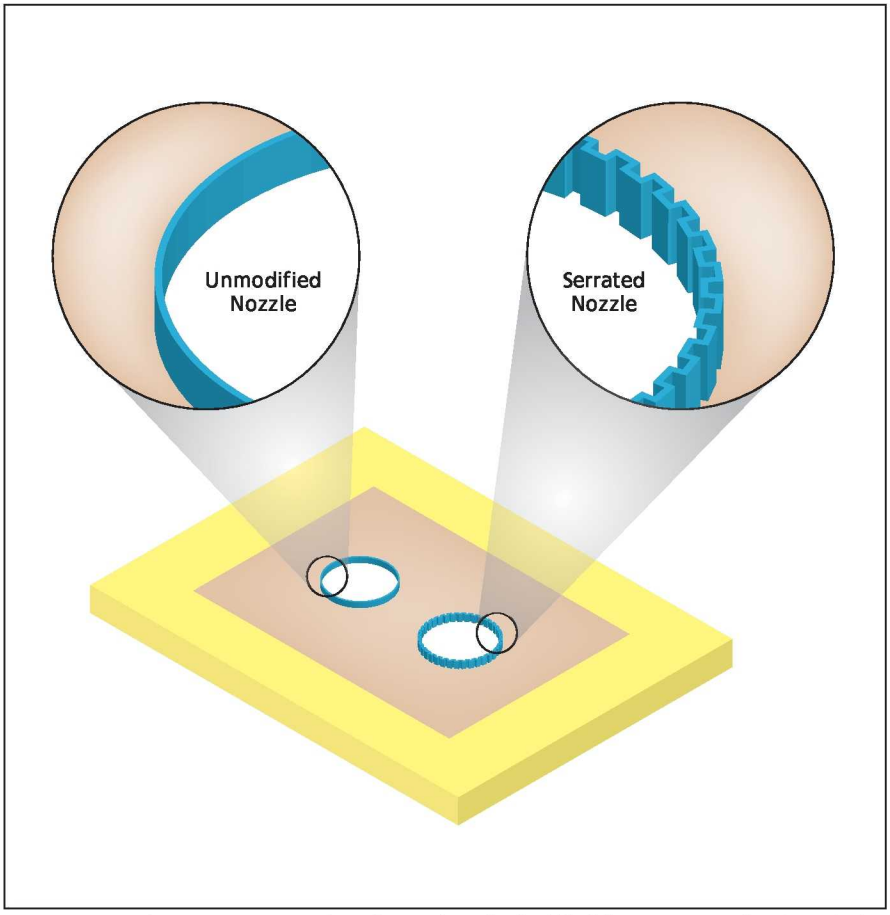


**Micromachined Serrations** on a nozzle surface reduce the liquid/solid contact area, thereby reducing the liquid/solid surface energy and thereby, further, reducing the liquid/nozzle attraction sufficiently to enable complete transfer of a liquid droplet from the nozzle to a nearby print surface.

The method was tested in experiments on soft printing of DNA solutions and of deionized water through 0.5-mm-diameter nozzles, of which some were not serrated, some were partially serrated, and some were fully serrated. In the nozzles without serrations, transfer was incomplete; that is, residual liquids remained in the nozzles after printing. However, in every nozzle in which at least half the inner surface was serrated, complete transfer of droplets to the print surface was achieved.

*This work was done by Chang-Jin "CJ" Kim of the University of California, Los Angeles, and Uichong Yi of Core Microsolutions, Inc. for Ames Research Center. For further information, contact the Ames Technology Partnerships Division at (650) 604-5761. ARC-15548-1*

# Turbomolecular Pumps for Holding Gases in Open Containers

**Thermal gas atoms would be trapped; much faster atoms would pass through.**

*Goddard Space Flight Center, Greenbelt, Maryland*

Proposed special-purpose turbomolecular pumps denoted turbotraps would be designed, along with mating open containers, to prevent the escape of relatively slowly (thermal) moving gas molecules from the containers while allowing atoms moving at much greater speeds to pass through. In the original intended applications, the containers would be electron-attachment cells, and the contained gases would be vapors of alkali metal atoms moving at thermal speeds that would be of the order of a fraction of 300 meters per second. These cells would be parts of apparatuses used to measure fluxes of neutral atoms incident at kinetic energies in the approximate range of 10 eV to 10 keV (corresponding to typical speeds of the order of 40,000 m/s and higher). The incident energetic neutral atoms would pass through the cells, wherein charge-exchange reactions with the alkali metal atoms would convert the neutral atoms to negative ions, which, in turn, could then be analyzed by use of conventional charged-particle optics.

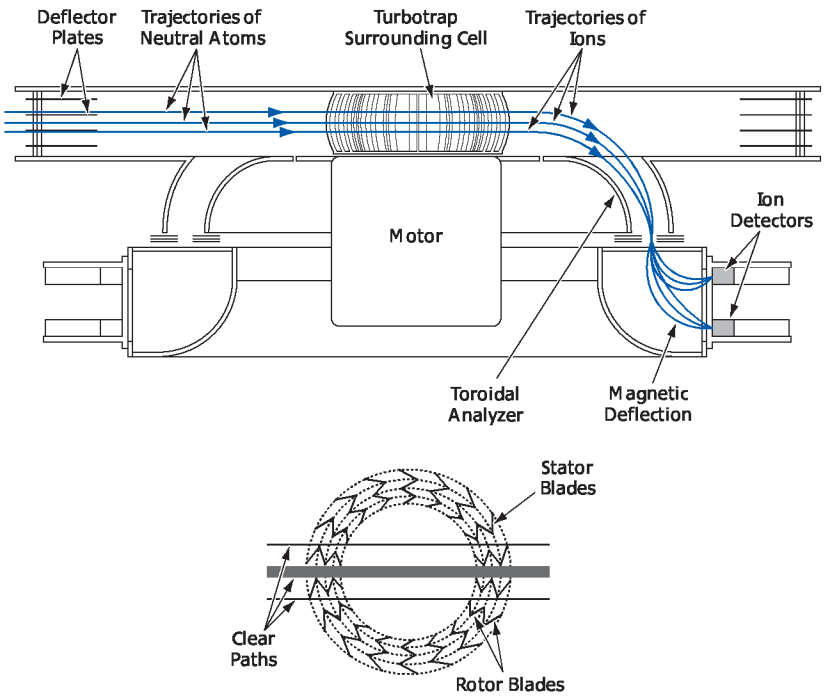


**Rotating and Stationary** concentric rows of blades would momentarily open paths along which high-speed atoms could travel through the cell bounded by the blade circles.

The figure depicts selected aspects of a turbotrap as part of such an apparatus. The turbotrap would exploit the large difference between the speed range of the incident energetic neutral atoms and the thermal speed range of the alkali metal atoms in the cell. The turbotrap would consist primarily of two or more rotating concentric rows of blades interspersed with two or more concentric stationary rows of blades. The relative positions of the blades, the sizes of the gaps between them, and the speed of rotation would be chosen so as to periodically open up one or more straight path(s) through the cell during a time interval long enough to allow the incident energetic neutral atoms to pass through but short enough so that there would be no clear path through the cell for the slower thermal alkali metal atoms. Moreover, the blades would be shaped and oriented to pump most of the incident thermal atoms back into the cell.

The feasibility of several turbotrap designs has been tentatively demonstrated by means of computational simulations. For example, in the case of one design involving two rows of stationary vanes and two rows of blades on a circle of about 10-cm diameter, a gap of 0.5 cm between blades, 50-percent open area, and a rotational speed of 32,000 rpm, the simulation showed that >99 percent of alkali metal atoms entering the turbotrap would be returned to the cell. The rotational speed in this example is well within that attainable by exploiting recent developments in the technological disciplines of reaction wheels, gyroscopes, and conventional turbomolecular pumps.

*This work was done by John W. Keller of Goddard Space Flight Center and John E. Lorenz of Litton Industries. Further information is contained in a TSP (see page 1).* GSC-14402-1

# Triaxial Swirl Injector Element for Liquid-Fueled Engines

**The design is amenable to low-cost production.**

*Marshall Space Flight Center, Alabama*

A triaxial injector is a single bi-propellant injection element located at the center of the injector body. The injector element consists of three nested, hydraulic swirl injectors. A small portion of the total fuel is injected through the central hydraulic injector, all of the oxidizer is injected through the middle concentric hydraulic swirl injector, and the balance of the fuel is injected through an outer concentric injection system. The configuration has been

shown to provide good flame stabilization and the desired fuel-rich wall boundary condition.

The injector design is well suited for preburner applications. Preburner injectors operate at extreme oxygen-to-fuel mass ratios, either very rich or very lean. The goal of a preburner is to create a uniform drive gas for the turbomachinery, while carefully controlling the temperature so as not to stress or damage turbine blades. The triaxial injector concept permits the lean propellant to be sandwiched between two layers of the rich propellant, while the hydraulic atomization characteristics of the swirl injectors promote interpropellant mixing and, ultimately, good combustion efficiency. This innovation is suited to a wide range of liquid oxidizer and liquid fuels, including hydrogen, methane, and kerosene.

Prototype testing with the triaxial swirl injector demonstrated excellent injector and combustion chamber thermal compatibility and good combustion performance, both at levels far superior to a pintle injector. Initial testing with the prototype injector demonstrated over 96-percent combustion efficiency. The design showed excellent high-frequency combustion stability characteristics with oxygen and kerosene propellants. Unlike the more conventional pintle injector, there is not a large bluff body that must be cooled. The absence of a protruding center body enhances the thermal durability of the triaxial swirl injector.

The hydraulic atomization characteristics of the innovation allow the design to be rapidly scaled from small in-space applications [500–5,000 lbf (2.2–22.2 kN)] to large thrust engine applications [80,000 lbf (356 kN) and beyond]. The triaxial injector is also less sensitive to eccentricities, manufacturing tolerances, and gap width of many traditional coaxial and pintle injector designs.

The triaxial-injector injection orifice configuration provides for high injection stiffness. The low parts count and relatively large injector design features are amenable to low-cost production.

*This work was done by Jeff Muss of Sierra Engineering Inc. for Marshall Space Flight Center. For more information, contact Sammy Nabors, MSFC Commercialization Assistance Lead, at sammy.a.nabors@nasa.gov. Refer to MFS-32717-1.*

## Integrated Budget Office Toolbox

The Integrated Budget Office Toolbox (IBOT) combines budgeting, resource allocation, organizational funding, and reporting features in an automated, integrated tool that provides data from a single source for Johnson Space Center (JSC) personnel. Using a common interface, concurrent users can utilize the data without compromising its integrity. IBOT tracks planning changes and updates throughout the year using both phasing and POP-related (program-operating-plan-related) budget information for the current year, and up to six years out.

Separating lump-sum funds received from HQ (Headquarters) into separate labor, travel, procurement, Center G&A (general & administrative), and service-pool categories, IBOT creates a script that significantly reduces manual input time. IBOT also manages the movement of travel and procurement funds down to the organizational level and, using its integrated funds management feature, helps better track funding at lower levels. Third-party software is used to create integrated reports in IBOT that can be generated for plans, actuals, funds received, and other combinations of data that are currently maintained in the centralized format. Based on Microsoft SQL, IBOT incorporates generic budget processes, is transportable, and is economical to deploy and support.

*This program was written by Douglas A. Rushing, Chris Blakeley, Gerry Chapman, and Bill Robertson of Johnson Space Center and Allison Horton, Thomas Besser, and Debbie McCarthy of SAIC. Further information is contained in a TSP (see page 1).* MSC-24167-1

## PLOT3D Export Tool for Tecplot

The PLOT3D export tool for Tecplot solves the problem of modified data being impossible to output for use by another computational science solver. The PLOT3D Exporter add-on enables the use of the most commonly available visualization tools to engineers for output of a standard format. The exportation of PLOT3D data from Tecplot has far reaching effects because it allows for grid and solution manipulation within a graphical user interface (GUI) that is easily customized with macro language-based and user-developed GUIs. The add-on also enables the use of Tecplot as an interpolation tool for solution conversion between different grids of different types. This one add-on enhances the functionality of Tecplot so significantly, it offers the ability to incorporate Tecplot into a general suite of tools for computational science applications as a 3D graphics engine for visualization of all data.

Within the PLOT3D Export Add-on are several functions that enhance the operations and effectiveness of the add-on. Unlike Tecplot output functions, the PLOT3D Export Add-on enables the use of the zone selection dialog in Tecplot to choose which zones are to be written by offering three distinct options — output of active, inactive, or all zones (grid blocks). As the user modifies the zones to output with the zone selection dialog, the zones to be written are similarly updated. This enables the use of Tecplot to create multiple configurations of a geometry being analyzed. For example, if an aircraft is loaded with multiple deflections of flaps, by activating and deactivating different zones for a specific flap setting, new specific configurations of that aircraft can be easily generated by only writing out specific zones. Thus, if ten flap settings are loaded into Tecplot, the PLOT3D Export software can output ten different configurations, one for each flap setting.

*This work was done by Stephen Alter of Langley Research Center. Further information is contained in a TSP (see page 1).* LAR-17678-1

## Math Description Engine Software Development Kit

The Math Description Engine Software Development Kit (MDE SDK) can be used by software developers to make computer-rendered graphs more accessible to blind and visually-impaired users. The MDE SDK generates alternative graph descriptions in two forms: textual descriptions and non-verbal sound renderings, or sonification. It also enables display of an animated trace of a graph sonification on a visual graph component, with color and line-thickness options for users having low vision or color-related impairments. A set of accessible graphical user interface widgets is provided for operation by end users and for control of accessible graph displays.

Version 1.0 of the MDE SDK generates text descriptions for 2D graphs commonly seen in math and science curriculum (and practice). The mathematically rich text descriptions can also serve as a virtual math and science assistant for blind and sighted users, making graphs more accessible for everyone.

The MDE SDK has a simple application programming interface (API) that makes it easy for programmers and Web-site developers to make graphs accessible with just a few lines of code. The source code is written in Java for cross-platform compatibility and to take advantage of Java's built-in support for building accessible software application interfaces. Compiled-library and NASA Open Source versions are available with API documentation and Programmer's Guide at http:// prime.jsc.nasa.gov.

*This work was done by Robert O. Shelton of Johnson Space Center, Stephanie L. Smith and Dan E. Dexter of L-3 Communications Corp., and Terry R. Hodgson of Indyne, Inc. Further information is contained in a TSP (see page 1).* MSC-24139-1

## Astronaut Office Scheduling System Software

AOSS is a highly efficient scheduling application that uses various tools to schedule astronauts' weekly appointment information. This program represents an integration of many technologies into a single application to facilitate schedule sharing and management. It is a Windows-based application developed in Visual Basic. Because the NASA standard office automation load environment is Microsoft-based, Visual Basic provides AOSS developers with the ability to interact with Windows collaboration components by accessing objects models from applications like Outlook and Excel. This also gives developers the ability to create newly customizable components that perform specialized tasks pertaining to scheduling reporting inside the application. With this capability, AOSS can perform various asynchronous tasks, such as gathering/ sending/ managing astronauts' schedule information directly to their Outlook calendars at any time. AOSS users use

this specific appointment information entered in the application to generate reports and to keep track of active NASA astronauts' whereabouts at all times.

AOSS can send or retrieve astronauts' schedule information via their individual Outlook calendars with a two-part process called PUSH and PULL. This process, along with weekly operational procedures agreed to by the users and current astronaut corps staff, delivers optimal scheduling processing performance. AOSS also provides the ability to create reports, statistics, and situation information for many NASA offices. Displays of the software are designed to be functional and familiar by using the same format design to ensure ease of use.

The software is composed of three main components — AOSS Application, AOSS Web, and AOSS Database. In the application, this is the main data entry point where most of the AOSS-typical transactions occur. AOSS users and the AOSS application perform data manipulation, reporting, and changes here. The application is the main lifeline between the user and the database. The AOSS Web function allows users to use a Web browser environment to view information, print results, and transact with the results of data entered in the AOSS database. This component contains a mixture of html and asp pages.

The main operation of the database is to hold data entered through the application component and to provide secure access to this information by qualified AOSS users, customers, and management. The database was developed in SQL and is held within an SQL server database environment. Using this system eliminates the need to prepare paper schedules and the time it takes to distribute them to the astronauts as well as ensuring a faster delivery of updates and schedule changes.

*This work was done by Estevancio Brown of United Space Alliance for Johnson Space Center. Further information is contained in a TSP (see page 1).* **MSC-24384-1**

## ISS Solar Array Management

The International Space Station (ISS) Solar Array Management (SAM) software toolset provides the capabilities necessary to operate a spacecraft with complex solar array constraints. It monitors spacecraft telemetry and provides interpretations of solar array constraint data in an intuitive manner. The toolset provides extensive situational awareness to ensure mission success by analyzing power generation needs, array motion constraints, and structural loading situations.

The software suite consists of several components including samCS (constraint set selector), samShadyTimers (array shadowing timers), samWin (visualization GUI), samLock (array motion constraint computation), and samJet (attitude control system configuration selector). It provides high availability and uptime for extended and continuous mission support. It is able to support two-degrees-of-freedom (DOF) array positioning and supports up to ten simultaneous constraints with intuitive 1D and 2D decision support visualizations of constraint data. Display synchronization is enabled across a networked control center and multiple methods for constraint data interpolation are supported. Use of this software toolset increases flight safety, reduces mission support effort, optimizes solar array operation for achieving mission goals, and has run for weeks at a time without issues.

The SAM toolset is currently used in ISS real-time mission operations.

*This work was done by James P. Williams, Keith D. Martin, Justin R. Thomas, and Samuel Caro of United Space Alliance for Johnson Space Center. Further information is contained in a TSP (see page 1).* **MSC-24425-1**

## Probabilistic Structural Analysis Program

NASA/ NESSUS 6.2c is a general-purpose, probabilistic analysis program that computes probability of failure and probabilistic sensitivity measures of engineered systems. Because NASA/ NESSUS uses highly computationally efficient and accurate analysis techniques, probabilistic solutions can be obtained even for extremely large and complex models. Once the probabilistic response is quantified, the results can be used to support risk-informed decisions regarding reliability for safety-critical and one-of-a-kind systems, as well as for maintaining a level of quality while reducing manufacturing costs for larger-quantity products. NASA/ NESSUS has been successfully applied to a diverse range of problems in aerospace, gas turbine engines, biomechanics, pipelines, defense, weaponry, and infrastructure.

This program combines state-of-the-art probabilistic algorithms with general-purpose structural analysis and lifting methods to compute the probabilistic response and reliability of engineered structures. Uncertainties in load, material properties, geometry, boundary conditions, and initial conditions can be simulated. The structural analysis methods include non-linear finite-element methods, heat-transfer analysis, polymer/ ceramic matrix composite analysis, monolithic (conventional metallic) materials life-prediction methodologies, boundary element methods, and user-written subroutines. Several probabilistic algorithms are available such as the advanced mean value method and the adaptive importance sampling method. NASA/ NESSUS 6.2c is structured in a modular format with 15 elements.

*This work was done by Shantaram S. Pai, Christos C. Chamis, Pappu L. N. Murthy, and George L. Stefko of Glenn Research Center; David S. Riha and Ben H. Thacker of Southwest Research Institute; Vinod K. Nagpal of N& R Engineering and Subodh K. Mital of the University of Toledo. FFurther information is contained in a TSP (see page 1).*

*Inquiries concerning rights for the commercial use of this invention should be addressed to NASA Glenn Research Center, Innovative Partnerships Office, Attn: Steve Fedor, Mail Stop 4–8, 21000 Brookpark Road, Cleveland, Ohio 44135. Refer to LEW-18229-1*

## SPOT Program

A Spacecraft Position Optimal Tracking (SPOT) program was developed to process Global Positioning System (GPS) data, sent via telemetry from a spacecraft, to generate accurate navigation estimates of the vehicle position and velocity (state vector) using a Kalman filter. This program uses the GPS onboard receiver measurements to sequentially calculate the vehicle state vectors and provide this information to ground flight controllers. It is the first real-time ground-based shuttle navigation application using onboard sensors. The program is compact, portable, self-contained, and can run on a variety of UNIX or Linux computers.

The program has a modular object-oriented design that supports application-specific plugins such as data corruption remediation pre-processing and remote graphics display. The Kalman filter is extensible to additional sensor types or force models. The Kalman filter design is also strong against data dropouts because it uses physical models from state and covariance propagation in the absence of data.

The design of this program separates the functionalities of SPOT into six dif-

ferent executable processes. This allows for the individual processes to be connected in an *a la carte* manner, making the feature set and executable complexity of SPOT adaptable to the needs of the user. Also, these processes need not be executed on the same workstation. This allows for communications between SPOT processes executing on the same Local Area Network (LAN). Thus, SPOT can be executed in a distributed sense with the capability for a team of flight controllers to efficiently share the same trajectory information currently being computed by the program.

SPOT is used in the Mission Control Center (MCC) for Space Shuttle Program (SSP) and International Space Station Program (ISSP) operations, and can also be used as a post-flight analysis tool. It is primarily used for situational awareness, and for contingency situations.

*This work was done by Jason T. Smith of Johnson Space Center and Sam J. Welsh, Antonio L. Farinetti, Tim Wegner, James Blakeslee, Toni F. Deboeck, Daniel Dyer, Bryan M. Corley, Jarmaine Ollivierre, Leonard Kramer, Patrick L. Zimmerman, and Reshma Khatri of United Space Alliance. Further information is contained in a TSP (see page 1).* MSC-24482-1

## Integrated Hybrid System Architecture for Risk Analysis

A conceptual design has been announced of an expert-system computer program, and the development of a prototype of the program, intended for use as a project-management tool. The program integrates schedule and risk data for the purpose of determining the schedule applications of safety risks and, somewhat conversely, the effects of changes in schedules on changes on safety. It is noted that the design has been delivered to a NASA client and that it is planned to disclose the design in a conference presentation.

*This work was done by Gary P. Moynihan, Daniel J. Fonseca, and Paul S. Ray of the University of Alabama for Johnson Space Center. For further information, contact the JSC Innovation Partnerships Office at (281) 483-3809.*

*The University of Alabama has requested permission to assert copyright for the software code.* MSC-23809-1

# System for Packaging Planetary Samples for Return to Earth

**System completes all the necessary steps for proper preservation.**

*NASA's Jet Propulsion Laboratory, Pasadena, California*

A system is proposed for packaging material samples on a remote planet (especially Mars) in sealed sample tubes in preparation for later return to Earth. The sample tubes (Figure 1) would comprise (1) tubes initially having open tops and closed bottoms; (2) small, bellowslike collapsible bodies inside the tubes at their bottoms; and (3) plugs to be eventually used to close the tops of the tubes. The top inner surface of each tube would be coated with solder. The side of each plug, which would fit snugly into a tube, would feature a solder-filled ring groove. The system would include equipment for storing, manipulating, filling, and sealing the tubes.

The containerization system (see Figure 2) will be organized in stations and will include: the storage station, the loading station, and the heating station. These stations can be structured in circular or linear pattern to minimize the manipulator complexity, allowing for compact design and mass efficiency. The manipulation of the sample tube between stations is done by a simple manipulator arm. The storage station contains the unloaded sample tubes and the plugs before sealing as well as the sealed sample tubes with samples after loading and sealing. The chambers at the storage station also allow for plug insertion into the sample tube. At the loading station the sample is poured or inserted into the sample tube and then the tube is topped off. At the heating station the plug is heated so the solder ring melts and seals the plug to the sample tube.

The process is performed as follows: Each tube is filled or slightly overfilled with sample material and the excess sample material is wiped off the top. Then, the plug is inserted into the top section of the tube packing the sample material against the collapsible bellowslike body allowing the accommodation of the sample volume. The plug and the top of the tube are heated momentarily to melt the solder in order to seal the tube.

*This work was done by Mircea Badescu, Yoseph Bar-Cohen, Paul G. Backes, Stewart Sherrit, Xiaoqi Bao, and James S. Scott of Caltech for NASA's Jet Propulsion Laboratory. Further information is contained in a TSP (see page 1).* NPO-46089

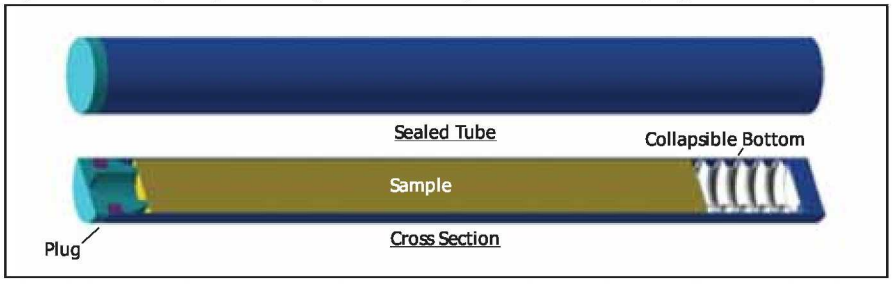


Figure 1: A **Sample Tube** is shown with collapsible bottom (on the right), sample, and sealed plug.


Figure 2: **Containerization System** includes loading, heating/sealing, and storage stations.

# Offset Compound Gear Drive

**A 50-percent reduction ratio is achieved with two stages utilizing four gears.**

*John H. Glenn Research Center, Cleveland, Ohio*

The Offset Compound Gear Drive is an in-line, discrete, two-speed device utilizing a special offset compound gear that has both an internal tooth configuration on the input end and external tooth configuration on the output end, thus allowing it to mesh in series, simultaneously, with both a smaller external tooth input gear and a larger internal tooth output gear. This unique geometry and offset axis permits the compound gear to mesh with the smaller diameter input gear and the larger diameter output gear, both of which are on the same central, or primary, centerline. This configuration results in a compact in-line reduction gear set consisting of fewer gears and bearings than a conventional planetary gear train. Switching between the two output ratios is accomplished through a main control clutch and sprag. Power flow to the above is transmitted through concentric power paths.

Low-speed operation is accomplished in two meshes. For the purpose of illustrating the low-speed output operation, the following example pitch diameters

are given. A 5.0 pitch diameter (PD) input gear to 7.50 PD (internal tooth) intermediate gear (0.667 reduction mesh), and a 7.50 PD (external tooth) intermediate gear to a 10.00 PD output gear (0.750 reduction mesh). Note that it is not required that the intermediate gears on the offset axis be of the same diameter. For this example, the resultant low-speed ratio is 2:1 (output speed = 0.500; product of stage one 0.667 reduction and stage two 0.750 stage reduction). The design is not restricted to the example pitch diameters, or output ratio. From the output gear, power is transmitted through a hollow drive shaft, which, in turn, drives a sprag during which time the main clutch is disengaged.

High-speed operation is direct-drive (1:1) through the main clutch. During this mode of operation, the above gear train free-wheels the overrunning sprag. A slight reduction in input speed is required to overrun the sprag. The above gear train always spins.

The configuration was conceived to meet a rotorcraft drive design objective to provide a 50-percent reduction ratio. The configuration does so in two stages, or meshes, utilizing only three gears replacing multiple planet gears required in conventional planetary stages. A same-direction 50-percent reduction is not possible with a single-stage simple planetary gear configuration.

In addition, ratios other than 50 percent can be configured to meet specific design requirements. This configuration overcomes a technical design challenge of configuring a simple and robust two-speed/ variable-speed driveline transmission that is lightweight yet capable of transferring high power at high speed for next-generation rotary wing aircraft, which are forecast to require speed range variations on the order of 50 percent.

*This work was done by Mark A. Stevens of Glenn Research Center, and Robert F. Handschuh and David G. Lewicki of U.S. Army Research Laboratory, Vehicle Technology Directorate, (located at Glenn Research Center). Further information is contained in a TSP (see page 1).*

*Inquiries concerning rights for the commercial use of this invention should be addressed to NASA Glenn Research Center, Innovative Partnerships Office, Attn: Steve Fedor, Mail Stop 4–8, 21000 Brookpark Road, Cleveland, Ohio 44135. Refer to LEW-18340-1.*

# Low-Dead-Volume Inlet for Vacuum Chamber

*John F. Kennedy Space Center, Florida*

Gas introduction from near-ambient pressures to high vacuum traditionally is accomplished either by multi-stage differential pumping that allows for very rapid response, or by a capillary method that allows for a simple, single-stage introduction, but which often has a delayed response. Another means to introduce the gas sample is to use the multi-stage design with only a single stage. This is accomplished by using a very small conductance limit. The problem with this method is that a small conductance limit will amplify issues associated with dead-volume.

As a result, a high-vacuum gas inlet was developed with low dead-volume, allowing the use of a very low conductance limit interface. Gas flows through the ConFlat flange at a relatively high flow rate at orders of magnitude greater than through the conductance limit. The small flow goes through a conductance limit that is a double-sided ConFlat.

*This work was done by Guy Naylor and C. Arkin of ASRC Aerospace Corporation for Kennedy Space Center. For further information, contact the Kennedy Innovative Partnerships Program Office at (321) 861-7158. KSC-13317*

# Simple Check Valves for Microfluidic Devices

**No additional materials or fabrication steps are necessary.**

*NASA's Jet Propulsion Laboratory, Pasadena, California*

A simple design concept for check valves has been adopted for microfluidic devices that consist mostly of (1) deformable fluorocarbon polymer membranes sandwiched between (2) borosilicate float glass wafers into which channels, valve seats, and holes have been etched. The first microfluidic devices in which these check valves are intended to be used are micro-capillary electrophoresis (microCE) devices undergoing development for use on Mars in detecting compounds indicative of life. In this application, it will be necessary to store some liquid samples in reservoirs in the devices for subsequent laboratory analysis, and check valves are needed to prevent cross-contamination of the samples. The simple check-valve design concept is also applicable to other microfluidic devices and to fluidic devices in general.

These check valves are simplified microscopic versions of conventional rubber-flap check valves that are parts of numerous industrial and consumer products. These check valves are fabricated, not as separate components, but as integral parts of microfluidic devices. A check valve according to this concept consists of suitably shaped portions of a deformable membrane and the two glass wafers between which the membrane is sandwiched (see figure). The valve flap is formed by making an approximately semicircular cut in the membrane. The flap is centered over a hole in the lower glass wafer, through which hole the liquid in question is intended to flow upward into a wider hole, channel, or reservoir in the upper glass wafer. The radius of the cut exceeds the radius of the hole by an amount large enough to prevent settling of the flap into the hole. As in a conventional rubber-flap check valve, back pressure in the liquid pushes the flap against the valve seat (in this case, the valve seat is the adjacent surface of the lower glass wafer), thereby forming a seal that prevents backflow.

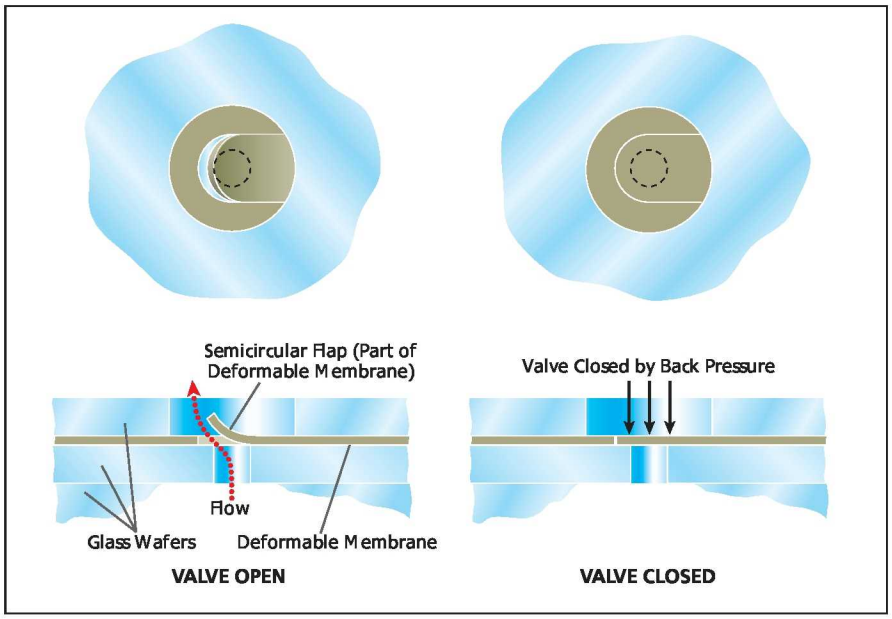


This **Microfluidic Check Valve** is a simplified version of a conventional rubber-flap check valve.

A typical sequence for fabricating a microfluidic device for the original intended microCE application includes the following steps:

1. Channels and valve seats are patterned in the two glass wafers between which the deformable membrane is to be sandwiched. (Altogether, there are three glass wafers, but the third wafer is irrelevant to the innovation described here.)
2. Holes are drilled through the wafers in predetermined locations for flowpaths.
3. The deformable membrane is fabricated.
4. Holes are punched in the membrane at locations matching those of holes, valve seats, and flow-channel orifices in the upper and lower glass plates. However, holes are not punched at locations where check valves are required.
5. At each check-valve location on the membrane, the check-valve flap is formed by use of an approximately semicircular punch. No membrane material is removed.

The ideal cut for forming a check-valve flap is an arc somewhat greater than a semicircle but less than a full circle. The resistance to flow through the check valve can be reduced by increasing the arc length of the punch. It is worth emphasizing that implementation of this concept entails nothing more than the use of additional punches for forming the flaps in the fabrication process.

*This work was done by Peter A. Willis, Harold F. Greer, and J. Anthony Smith of Caltech for NASA's Jet Propulsion Laboratory. Further information is contained in a TSP (see page 1).* *NPO-45933*

# A Capillary-Based Static Phase Separator for Highly Variable Wetting Conditions

## Commercially viable two-phase flow/ liquid management field applications have been developed for microgravity.

*Lyndon B. Johnson Space Center, Houston, Texas*

The invention, a static phase separator (SPS), uses airflow and capillary wetting characteristics to passively separate a two-phase (liquid and air) flow. The device accommodates highly variable liquid wetting characteristics. The resultant design allows for a range of wetting properties from about 0 to over 90° advancing contact angle, with frequent complete separation of liquid from gas observed when using appropriately scaled test conditions. Additionally, the design accommodates a range of air-to-liquid flow-rate ratios from only liquid flow to over 200:1 air-to-liquid flow rate.

The SPS uses a helix input section with an ice-cream-cone-shaped constant area cross section (see figure). The wedge portion of the cross section is on the outer edge of the helix, and collects the liquid via centripetal acceleration. The helix then passes into an increasing cross-sectional area vane region. The liquid in the helix wedge is directed into the top of capillary wedges in the liquid containment section. The transition from diffuser to containment section includes a 90° change in capillary pumping direction, while maintaining inertial direction. This serves to impinge the liquid into the two off-center symmetrical vanes by the airflow.

Rather than the airflow serving to shear liquid away from the capillary vanes, the design allows for further penetration of the liquid into the vanes by the air shear. This is

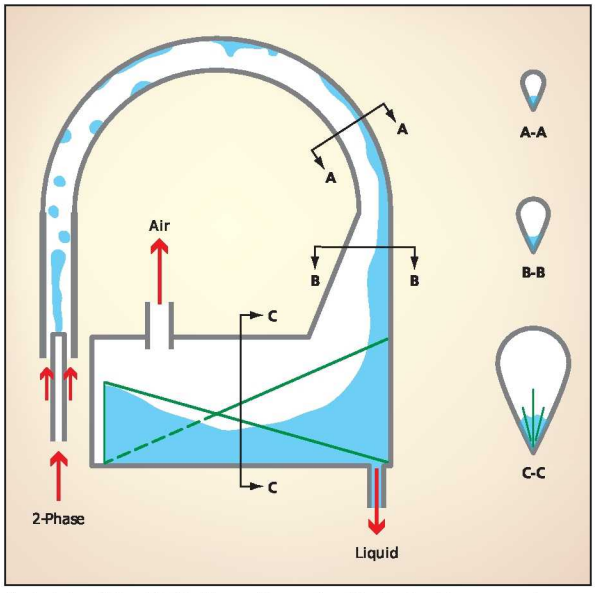


A sketch of the **Static Phase Separator** illustrates the geometry.

also assisted by locating the air exit ports downstream of the liquid drain port. Additionally, any droplets not contained in the capillary vanes are re-entrained downstream by a third opposing capillary vane, which directs liquid back toward the liquid drain port. Finally, the dual air exit ports serve to slow the airflow down, and to reduce the likelihood of shear. The ports are stove-piped into the cavity to form an unfriendly capillary surface for a wetting fluid to carryover. The liquid drain port is located at the start of the containment region, allowing for draining the bulk fluid in a continuous circuit.

The functional operation of the SPS involves introducing liquid flow (from a human body, a syringe, or other source) to the two-phase inlet while an air fan pulls on the air exit lines. The fan is operated until the liquid is fully introduced. The system is drained by negative pressure on the liquid drain lines when the SPS containment system is full.

*This work was done by Evan A. Thomas and John C. Graf of Johnson Space Center and Mark M. Weislogel, independent consultant. Further information is contained in a TSP (see page 1).*

*This invention is owned by NASA, and a patent application has been filed. Inquiries concerning nonexclusive or exclusive license for its commercial development should be addressed to the Patent Counsel, Johnson Space Center, (281) 483-1003. Refer to MSC-24441-1.*

## Gimballing Spacecraft Thruster

*Marshall Space Flight Center, Alabama*

A gimballing spacecraft reaction-control-system thruster was developed that consists of a small hydrogen/oxygen-burning rocket engine integrated with a Canfield joint. (Named after its inventor, a Canfield joint is a special gimbal mount that is strong and stable yet allows a wide range of motion.) One especially notable aspect of the design of this thruster is integration, into both the stationary legs and the moving arms of the Canfield joint, of the passages through which the hydrogen and oxygen flow to the engine. The thruster was assembled and subjected to tests in which the engine was successfully fired both with and without motion in the Canfield joint.

*This work was done by Tim Pickens and John Bossard of Orion Propulsion, Inc. for Marshall Space Flight Center. For further information, contact Sammy Nabors, MSFC Commercialization Assistance Lead, at sammy.a.nabors@nasa.gov. Refer to MFS-32520-1.*

## Finned Carbon-Carbon Heat Pipe With Potassium Working Fluid

**The heat pipe can be used in terrestrial power plants.**

*John H. Glenn Research Center, Cleveland, Ohio*

This elemental space radiator heat pipe is designed to operate in the 700 to 875 K temperature range. It consists of a C–C (carbon-carbon) shell made from poly-acrylonitride fibers that are woven in an angle interlock pattern and densified with pitch at high process temperature with integrally woven fins. The fins are 2.5 cm long and 1 mm thick, and provide an extended radiating surface at the colder condenser section of the heat pipe. The weave pattern features a continuous fiber bath from the inner tube surface to the outside edges of the fins to maximize the thermal conductance, and to thus minimize the temperature drop at the condenser end. The heat pipe and radiator element together are less than one-third the mass of conventional heat pipes of the same heat rejection surface area.

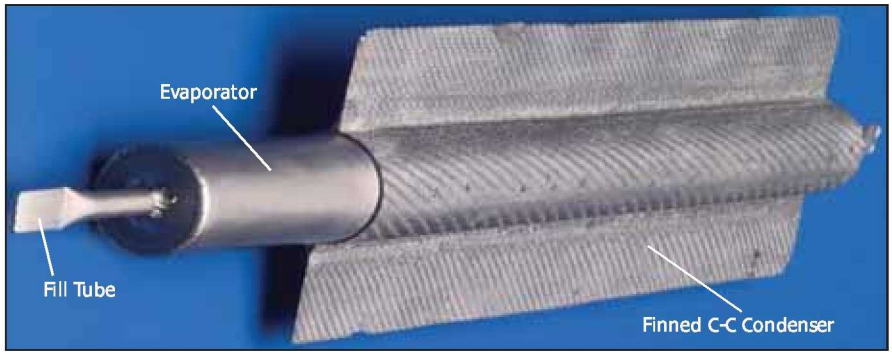


The finned **Carbon-Carbon Heat Pipe** is shown with an Nb-1Zr evaporator liner.

To prevent the molten potassium working fluid from eroding the C–C heat pipe wall, the shell is lined with a thin-walled, metallic tube liner (Nb-1 wt.% Zr), which is an integral part of a hermetic metal subassembly which is furnace-brazed to the inner surface of the C–C tube. The hermetic metal liner subassembly includes end caps and fill tubes fabricated from the same Nb-1Zr alloy. A combination of laser and electron beam methods is used to weld the end caps and fill tubes. A tungsten/inert gas weld seals the fill tubes after cleaning and charging the heat pipes with potassium.

The external section of this liner, which was formed by a "Uniscan" rolling process, transitions to a larger wall thickness. This section, which protrudes beyond the C–C shell, constitutes the "evaporator" part of the heat pipe, while the section inside the shell constitutes the condenser of the heat pipe (see figure). The metal liner contains a concentric tubular perforated wick sized and located to form an annu-

lar gap between itself and the inner surface of the liner. The wick is fabricated from molybdenum foil and contains evenly spaced circular perforations. One end of the wick is welded to the evaporator end cap, while the other end is left free.

During the fabrication process, the finned C–C shell condenser section is exposed to an atomic oxygen (AO) ion source for a total AO fluence of $4 \times 10^{20}$ atoms/ $cm^2$, thereby raising its surface emissivity to values between 0.85 and 0.90 at design operating temperature, thus reducing the radiator area required for a specified value of heat rejection to space. The prototype heat pipe performed well in initial low-power tests. Based on test results and computer modeling, the heat pipe should be capable of transporting heat at a rate of 900 W at evaporator temperatures in the 850 to 875 K range. Computer modeling also indicates that, if scaled up from a prototype length of 36 cm to a full design length of 91 cm, the heat pipe should be capable of transporting heat at a rate of 2.2 kW at the same evaporator temperature range. At its 1.45 kg/ $m^2$ specific mass for two-sided heat rejection, its power-to-mass ratio will be 6.5 kW/ kg.

*This work was done by Albert J. Juhasz of Glenn Research Center. Further information is contained in a TSP (see page 1).*

*Inquiries concerning rights for the commercial use of this invention should be addressed to NASA Glenn Research Center, Innovative Partnerships Office, Attn: Steve Fedor, Mail Stop 4–8, 21000 Brookpark Road, Cleveland, Ohio 44135. Refer to LEW-18307-1.*

# Lightweight Heat Pipes Made From Magnesium

*Lyndon B. Johnson Space Center, Houston, Texas*

Magnesium has shown promise as a lighter-weight alternative to the aluminum alloys now used to make the main structural components of axially grooved heat pipes that contain ammonia as the working fluid. Magnesium heat-pipe structures can be fabricated by conventional processes that include extrusion, machining, welding, and bending. The thermal performances of magnesium heat pipes are the same as those of equal-sized aluminum heat pipes. However, by virtue of the lower mass density of magnesium, the magnesium heat pipes weigh 35 percent less. Conceived for use aboard spacecraft, magnesium heat pipes could also be attractive as heat-transfer devices in terrestrial applications in which minimization of weight is sought: examples include radio-communication equipment and laptop computers.

*This work was done by John H. Rosenfeld, Sergei N. Zarembo, and G. Yale Eastman of Thermacore, Inc. for Johnson Space Center. Further information is contained in a TSP (see page 1).*

*In accordance with Public Law 96-517, the contractor has elected to retain title to this invention. Inquiries concerning rights for its commercial use should be addressed to:*

*Thermacore International, Inc.*
*780 Eden Rd.*
*Lancaster, PA 17601*
*Phone No.: (717) 569-6551*
*E-mail: info@thermacore.com*

*Refer to MSC-23397-1, volume and number of this* NASA Tech Briefs *issue, and the page number.*

# Ceramic Rail-Race Ball Bearings

## These bearings would tolerate dust better than conventional ball bearings.

*NASA's Jet Propulsion Laboratory, Pasadena, California*

Non-lubricated ball bearings featuring rail races have been proposed for use in mechanisms that are required to function in the presence of mineral dust particles in very low-pressure, dry environments with extended life. Like a conventional ball bearing, the proposed bearing would include an inner and an outer ring separated by balls in rolling contact with the races. However, unlike a conventional ball bearing, the balls would not roll in semi-circular or gothic arch race grooves in the rings: instead, the races would be shaped to form two or more rails (see figure). During operation, the motion of the balls would push dust particles into the spaces between the rails where the particles could not generate rolling resistance for the balls.

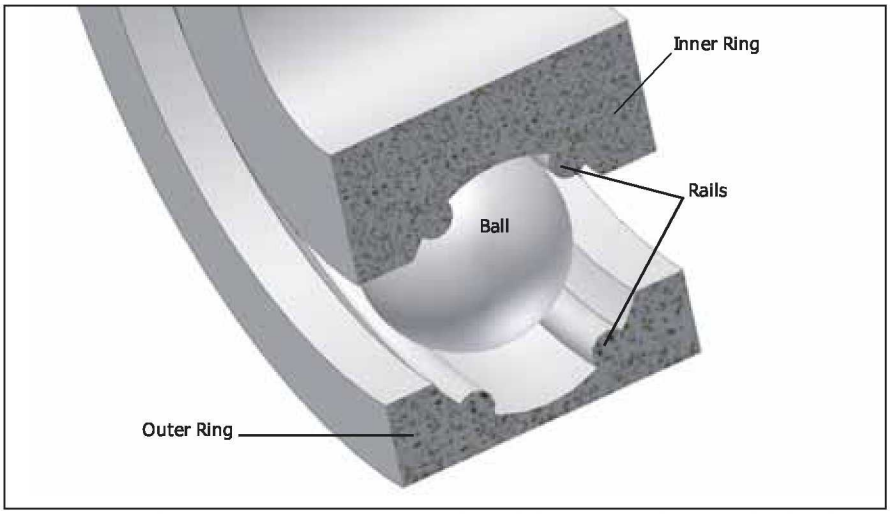


A **Ball Bearing as Proposed** would contain rail races instead of conventional races. Preferably, the balls, rings and rail-races would be made of a ceramic or similar hard material.

The rail and ball materials must have very high compressive strength, hardness, and wear resistance in order for the rail-race bearing to have a reasonable load capacity and be able to operate in the presence of the dust particles with minimal wear. Preferably, both the rails and the balls would be made of ceramics identical or similar to those now used in some commercially available bearings. These ceramics have strengths and hardnesses greater than those of the dust particles. The rails would be integral with the rings and formed by grinding ceramic ring blanks.

*This work was done by Mark A. Balzer, Greg S. Mungas, and Gregory H. Peters of Caltech for NASA's Jet Propulsion Laboratory.*

*In accordance with Public Law 96-517, the contractor has elected to retain title to this invention. Inquiries concerning rights for its commercial use should be addressed to:*

*Innovative Technology Assets Management*
*JPL*
*Mail Stop 202-233*
*4800 Oak Grove Drive*
*Pasadena, CA 91109-8099*
*E-mail: iaoffice@jpl.nasa.gov*

*Refer to NPO-44908, volume and number of this* NASA Tech Briefs *issue, and the page number.*

# Improved OTEC System for a Submarine Robot

**This system supplants a related, previously proposed OTEC system.**

*NASA's Jet Propulsion Laboratory, Pasadena, California*

An ocean thermal energy conversion (OTEC), now undergoing development, is a less-massive, more-efficient means of exploiting the same basic principle as that of the proposed system described in "Alternative OTEC Scheme for a Submarine Robot" (NPO-43500), *NASA Tech Briefs*, Vol. 33, No. 1 (January 2009), page 50. The proposed system as described previously would be based on the thawing-expansion/ freezing-contraction behavior of a wax or perhaps another suitable phase-change material (PCM). The power generated by the system would be used to recharge the batteries in a battery-powered unmanned underwater vehicle [UUV (essentially, a small exploratory submarine robot)] of a type that has been deployed in large numbers in research pertaining to global warming. A UUV of this type travels between the ocean surface and depths, measuring temperature and salinity.

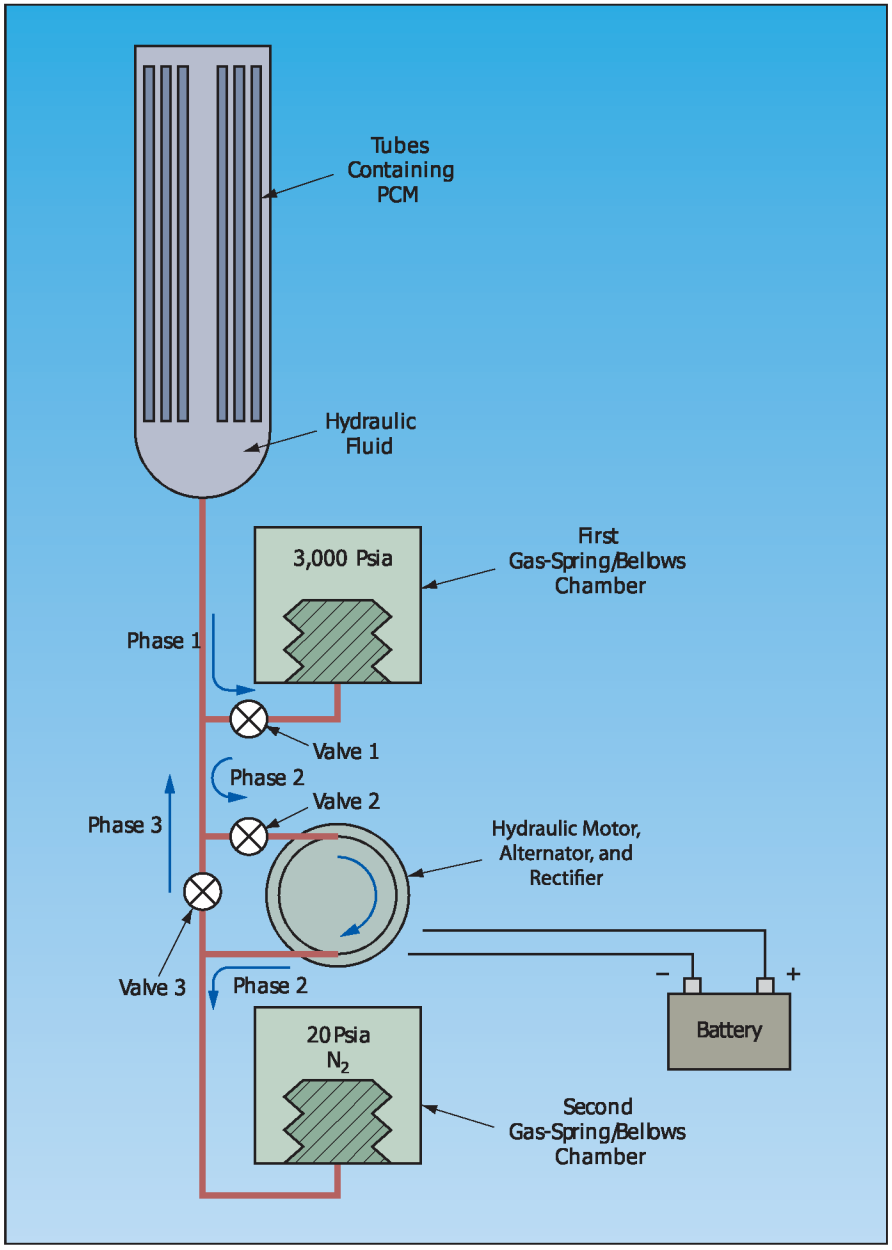


The **PCM Expands and Contracts** upon melting near the ocean surface and freezing at depth, respectively. The expansion and contraction causes the hydraulic fluid to flow cyclically through the hydraulic motor to drive the alternator to charge the battery.

At one phase of its operational cycle, the previously proposed system would utilize the surface ocean temperature (which lies between 15 and 30 °C over most of the Earth) to melt a PCM that has a melting/ freezing temperature of about 10 °C. At the opposite phase of its operational cycle, the system would utilize the lower ocean temperature at depth (e.g., between 4 and 7 °C at a depth of 300 m) to freeze the PCM. The melting or freezing would cause the PCM to expand or contract, respectively, by about 9 volume percent. The PCM would be contained in tubes that would be capable of expanding and contracting with the PCM. The PCM-containing tubes would be immersed in a hydraulic fluid. The expansion and contraction would drive a flow of the hydraulic fluid against a piston that, in turn, would push a rack-and-pinion gear system to spin a generator to charge a battery.

The present system was conceived because the previously proposed system was found to be too heavy and inefficient for the intended application. The main difference between the present and previously proposed systems is that in the present system, the flow of hydraulic fluid drives a hydraulic motor instead of a piston.

The operational cycle of the present system involves three phases of flow of the hydraulic fluid and is best understood by reference to the figure. In phase 1, near the ocean surface, valve 1 is held open and valves 2 and 3 are held closed, and the expansion of PCM upon heating to >10 °C pushes the hydraulic fluid through valve 1 into the bellows in a gas-spring/ bellows chamber, charging

the chamber to an absolute pressure of about 3 kpsi (≈21 MPa). In phase 2, valve 2 is opened, allowing the pressurized hydraulic fluid to flow through the hydraulic motor and into the bellows in a second, lower-pressure gas-spring/ bellows chamber. Upon completion of this flow, valves 1 and 2 are closed and valve 3 opened in anticipation of phase 3. In phase 3, which takes place upon cooling to <10 °C at depth, contraction of the PCM upon freezing reverses the pressure gradient in the plumbing, causing the hydraulic fluid to flow from the second gas-spring/ bellows chamber back to the chamber containing the PCM.

*This work was done by Yi Chao, Jack Jones, and Thomas Valdez of Caltech for NASA's Jet Propulsion Laboratory. Further information is contained in a TSP (see page 1).*

*In accordance with Public Law 96-517, the contractor has elected to retain title to this invention. Inquiries concerning rights for its commercial use should be addressed to:*

*Innovative Technology Assets Management*
*JPL*
*Mail Stop 202-233*
*4800 Oak Grove Drive*
*Pasadena, CA 91109-8099*
*E-mail: iaoffice@jpl.nasa.gov*

*Refer to NPO-45404, volume and number of this* NASA Tech Briefs *issue, and the page number.*

# Reflector Surface Error Compensation in Dual-Reflector Antennas

**Real-time detection and compensation of reflector surface errors is enabled for large reflector antennas such as inflatable antennas for Earth and space science applications.**

*NASA's Jet Propulsion Laboratory, Pasadena, California*

By probing the field on a small subreflector at a minimal number of points, the main reflector surface errors can be obtained and subsequently used to design a phase-correction subreflector that can compensate for main reflector errors. The compensating phase-error profile across the subreflector can be achieved either by a surface deformation or by the use of an array of elements such as patch antennas that can cause a phase shift between the incoming and outgoing fields. The second option is of primary interest here, but the methodology can be applied to either case. The patch array is most easily implemented on a planar surface. Therefore, the example of a flat subreflector and a parabolic main reflector (a Newtonian dual reflector system) is considered in this work.

The subreflector is assumed to be a reflector array covered with patch elements. The phase variation on a subreflector can be detected by a small number of receiving patch elements (probes). By probing the phase change at these few selected positions on the subreflector, the phase error over the entire surface can be recovered and used to change the phase of all the patch elements covering the subreflector plane to compensate for main reflector errors. This is accomplished by using a version of sampling theorem on the circular aperture.

The sampling is performed on the phase-error function on the circular aperture of the main reflector by a method developed using Zernike polynomials. This method is based upon and extended from a theory previously proposed and applied to reflector aperture integration. This sampling method provides for an exact retrieval of the coefficients of up to certain orders in the expansion of the phase function, from values on a specifically calculated set of points in radial and azimuthal directions in the polar coordinate system, on the circular reflector aperture. The corresponding points on the subreflector are then obtained and, by probing the fields at these points, a set of phase values is determined that is then transferred back to the main reflector aperture for recovering the phase function. Once this function is recovered, the corresponding phase function on the subreflector is calculated and used to compensate for main reflector surface errors. In going back and forth between sub and main reflectors, geometrical (ray) optics is employed, which even though it ignores edge diffraction and other effects, is shown to be accurate for phase recovery.

This work has direct application to reflector antennas, particularly large spaceborne inflatable antennas at X, Ka, and higher frequency bands. This method can also be effective in scanning or multi-beam reflector antenna systems in which the range of scan can be increased by phase-error compensation on the subreflector.

*This work was done by Vahraz Jamnejad and William Imbriale of Caltech for NASA's Jet Propulsion Laboratory. For more information, contact iaoffice@jpl.nasa.gov. NPO-45373*

# Enriched Storable Oxidizers for Rocket Engines

**These oxidizers could be stored at room temperature.**

*Marshall Space Flight Center, Alabama*

The name "enriched storable oxidizers" (ESOs) has been coined for a family of optimized mixtures of between two and four oxidizer fluids. For most applications, the constituents of these mixtures would be nitrogen tetroxide ($N_2O_4$), nitrous oxide ($N_2O$), and nitrogen dioxide ($NO_2$); in some applications, the mixtures might include inhibited red fuming nitric acid [IRFN (which consists of red fuming nitric acid to which some hydrogen fluoride is added to reduce its corrosive effect]. The optimum proportions of these constituents would be different for different applications. ESOs were originally proposed for use in spacecraft and launch-rocket propulsion systems: ESOs could be especially useful in advanced spacecraft propulsion systems that could operate in multiple modes. ESOs might also

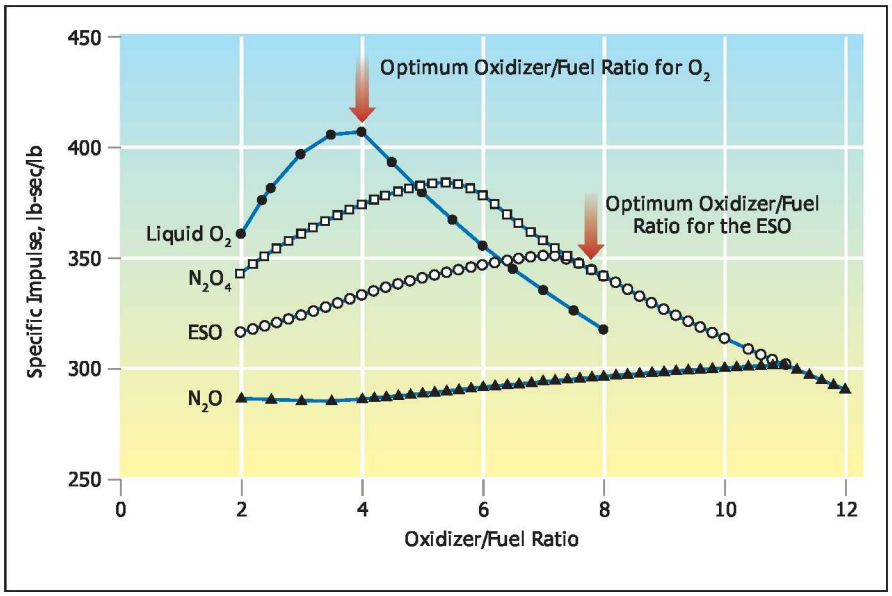


**Specific Impulse Versus Oxidizer/Fuel Ratio** was calculated for methane burned with either (1) $N_2O_4$, (2) an ESO comprising a mixture of 65 mole percent of $N_2O$ with 35 mole percent of $N_2O_4$, (3) $N_2O$, or (4) liquid $O_2$. The combustion-chamber and exit pressures used in the calculations were 1,000 psi (≈6.89 MPa) and 0.05 psi (≈345 Pa), respectively. Stoichiometry favors higher oxidizer/fuel ratios for the ESO than for liquid $O_2$; this is fortuitous because, as the corresponding plots show, the higher mixture ratio yields higher specific impulse.

be useful in special terrestrial applications that could include ramjet and scramjet aircraft engines.

ESOs would offer an attractive alternative to liquid oxygen and other previously known oxidizer fluids, including the individual constituents of these mixtures:

- Unlike liquid oxygen and fluorine-based oxidizers, which must be stored under cryogenic conditions, ESOs could be stored at room temperature.
- In comparison with most previously known oxidizer fluids other than oxygen, nitrous oxide, and nitrogen peroxide, ESOs would be less toxic.
- In comparison with most previously known oxidizer fluids other than nitrous oxide, ESOs would be less corrosive, and would be more chemically stable in storage.

Calculations have shown that ESOs would offer high energy densities and that specific-impulse levels attainable by use of ESOs would approach those attainable by use of liquid oxygen with two hydrocarbon fuels — RP-1 (rocket propellant 1, which is similar to kerosene) and methane (see figure). ESOs would be hypergolic or nearly hypergolic with methane and RP-1 and with other fuels that include Jet-A (also similar to kerosene), hydrazine, and monomethyl hydrazine. A computational simulation has predicted that only benign exhaust products would result from burning methane or RP-1 with one of the ESOs (a mixture of 35 mole percent of $N_2O_4$ with 65 mole percent of $N_2O$): These exhaust products would be primarily $CO_2$, $H_2O$, and $N_2$, plus very small amounts of $O_2$.

*This work was done by R. L. Sackheim of Marshall Space Flight Center and J. R. Herdy, Jr., of Qualis Corp.*

*This invention is owned by NASA, and a patent application has been filed. For further information, contact Sammy Nabors, MSFC Commercialization Assistance Lead, at sammy.a.nabors@nasa.gov. Refer to MFS-32407-1.*

# Planar Submillimeter-Wave Mixer Technology With Integrated Antenna

## This technology can be used for terahertz radar imagers and in testing of quantum cascade lasers.

*NASA's Jet Propulsion Laboratory, Pasadena, California*

High-performance mixers at terahertz frequencies require good matching between the coupling circuits such as antennas and local oscillators and the diode embedding impedance. With the availability of amplifiers at submillimeter wavelengths and the need to have multi-pixel imagers and cameras, planar mixer architecture is required to have an integrated system. An integrated mixer with planar antenna provides a compact and optimized design at terahertz frequencies. Moreover, it leads to a planar architecture that enables efficient interconnect with submillimeter-wave amplifiers.

In this architecture, a planar slot antenna is designed on a thin gallium arsenide (GaAs) membrane in such a way that the beam on either side of the membrane is symmetric and has good beam profile with high coupling efficiency. A coplanar waveguide (CPW) coupled Schottky diode mixer is designed and integrated with the antenna. In this architecture, the local oscillator (LO) is coupled through one side of the antenna and the RF from the other side, without requiring any beamsplitters or diplexers. The intermediate frequency (IF) comes out on a 50-ohm CPW line at the edge of the mixer chip, which can be wire-bonded to external circuits. This unique terahertz mixer has an integrated single planar antenna for coupling both the radio frequency (RF) input and LO injection without any diplexer or beamsplitters. The design utilizes novel planar slot antenna architecture on a 3-μm-thick GaAs membrane.

This work is required to enable future multi-pixel terahertz receivers for astrophysics missions, and lightweight and compact receivers for planetary missions to the outer planets in our solar system. Also, this technology can be used in terahertz radar imaging applications as well as for testing of quantum cascade lasers (QCLs).

*This work was done by Goutam Chattopadhyay, Imran Mehdi, John J. Gill, Choonsup Lee, and Nuria Llombart of Caltech for NASA's Jet Propulsion Laboratory and Bertrand Thomas of Oak Ridge Associated Universities. Further information is contained in a TSP (see page 1).* NPO-46880

# Widely Tunable Mode-Hop-Free External-Cavity Quantum Cascade Laser

**This technology is suitable for spectroscopic applications, multi-species trace-gas detection, and measurements of broadband absorbers.**

*Lyndon B. Johnson Space Center, Houston, Texas*

The external-cavity quantum cascade laser (EC-QCL) system is based on an optical configuration of the Littrow type. It is a room-temperature, continuous-wave, widely tunable, mode-hop-free, mid-infrared, EC-QCL spectroscopic source. It has a single-mode tuning range of 155 $cm^{-1}$ (≈8% of the center wavelength) with a maximum power of 11.1 mW and 182 $cm^{-1}$ (≈15% of the center wavelength), and a maximum power of 50 mW as demonstrated for 5.3 micron and 8.4 micron EC-QCLs, respectively. This technology is particularly suitable for high-resolution spectroscopic applications, multi-species trace-gas detection, and spectroscopic measurements of broadband absorbers.

Wavelength tuning of EC-QCL spectroscopic source can be implemented by varying three independent parameters of the laser: (1) the optical length of the gain medium (which, in this case, is equivalent to QCL injection current modulation), (2) the length of the EC (which can be independently varied in the Rice EC-QCL setup), and (3) the angle of beam incidence at the diffraction grating (frequency tuning related directly to angular dispersion of the grating). All three mechanisms of frequency tuning have been demonstrated and are required to obtain a true mode-hop-free laser frequency tuning.

The precise frequency tuning characteristics of the EC-QCL output have been characterized using a variety of diagnostic tools available at Rice University (e.g., a monochromator, FTIR spectrometer, and a Fabry-Perot spectrometer). Spectroscopic results were compared with available databases (such as HITRAN, PNNL, EPA, and NIST). These enable precision verification of complete spectral parameters of the EC-QCL, such as wavelength, tuning range, tuning characteristics, and line width.

The output power of the EC-QCL is determined by the performance of the QC laser chip, its operating conditions, and parameters of the QC laser cavity such as mirror reflectivity or intracavity losses. In order to maximize the output power, an analysis and optimization of the EC laser parameters has been performed. The parameters of the beam emitted from the gain medium, such as divergence angle, beam profile, and astigmatism, have been investigated. The gain medium has been fully characterized before and after each stage of modification. The main modification steps are coating one facet of the gain chip with a high reflectivity mirror and the other facet with an anti-reflection layer. Then the chip is mounted in the EC-QCL. The optomechanical design has been reviewed and improved to provide for precise collimation of the strongly divergent beam of the QCL and the tuning diffraction grating.

*This work was done by Gerard Wysocki, Robert F. Curl, and Frank K. Tittel of Rice University for Johnson Space Center. Further information is contained in a TSP (see page 1).*

*In accordance with Public Law 96-517, the contractor has elected to retain title to this invention. Inquiries concerning rights for its commercial use should be addressed to:*

*Rice University*
*6100 Main St.*
*Houston, TX 77005*

*Refer to MSC-24486-1, volume and number of this* NASA Tech Briefs *issue, and the page number.*

# Non-Geiger-Mode Single-Photon Avalanche Detector With Low Excess Noise

**Applications include quantum key distribution for the financial industry and photon-starved optical communications needs.**

*NASA's Jet Propulsion Laboratory, Pasadena, California*

This design constitutes a self-resetting (gain quenching), room-temperature operational semiconductor single-photon-sensitive detector that is sensitive to telecommunications optical wavelengths and is scalable to large areas (millimeter diameter) with high bandwidth and efficiencies.

The device can detect single photons at a 1,550-nm wavelength at a gain of $1 \times 10^6$. Unlike conventional single photon avalanche detectors (SPADs), where gain is an extremely sensitive function to the bias voltage, the multiplication gain of this device is stable at $1 \times 10^6$ over a wide range of bias from 30.2 to 30.9 V. Here, the multiplication gain is defined as the total number of charge carriers contained in one output pulse that is triggered by the absorption of a single photon. The statistics of magnitude of output signals also shows that the device has a very narrow pulse height distribution, which demonstrates a greatly suppressed gain fluctuation. From the histograms of both pulse height and pulse charge, the equivalent gain variance (excess noise) is between 1.001 and 1.007 at a gain of $1 \times 10^6$. With these advantages, the device holds promise to function as a PMT-like photon counter at a 1,550-nm wavelength.

The epitaxial layer structure of the device allows photons to be absorbed in the InGaAs layer, generating electron/hole (e-h) pairs. Driven by an electrical field in InGaAs, electrons are collected at the anode while holes reach the multiplication region (InAlAs p-i-n structure) and trigger the avalanche process. As a result, a large number of e-h pairs are created, and the holes move toward

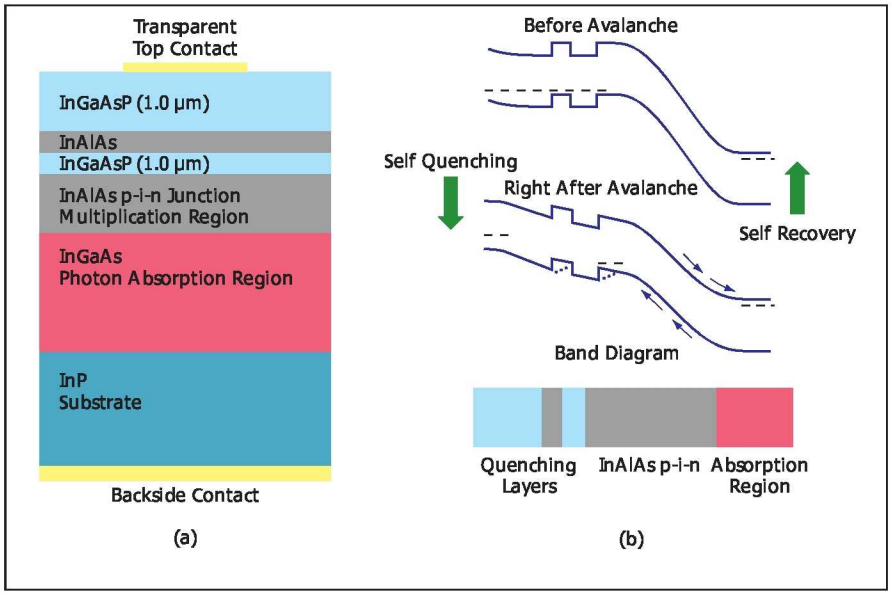


The schematic diagram of the **InGaAs-InAsAs SPAD Layer Structure** (a) and (b) the **Concept of Operation** for the structure showing the self-quenching and self-recovery processes.

the cathode. Holes created by the avalanche process gain large kinetic energy through the electric field, and are considered "hot". These hot holes are cooled as they travel across a p-InAlAs low field region, and are eventually blocked by energy barriers formed by the InGaAsP/ InAlAs heterojunctions.

The composition of the InGaAsP alloy was chosen to have an 80 meV valance band offset with InAlAs, which is high enough to hinder the transport of the already cooled holes. Being stopped by the energy barrier, holes are accumulated at the junctions to shield the electric field, resulting in a decrease of the electric field in the multiplication region. Because the impact ionization rate is extremely sensitive to the magnitude of the electric field, the field-screening effect drastically reduces the impact ionization rate and quenches the output signals.

After the avalanche pulse signal is self-quenched, the accumulated holes at the InGaAsP/ InAlAs interface escape the energy barrier through thermal excitation and tunneling and finally leave the device. The device is thus reset and ready for subsequent photon detection. This recovery time is controlled by the height of the energy barrier and the hole-cooling rate.

*This work was done by Kai Zhao and Yu-Hwa Lo of the University of California San Diego and William Farr of Caltech for NASA's Jet Propulsion Laboratory. Further information is contained in a TSP (see page 1).* *NPO-45801*

# Using Whispering-Gallery-Mode Resonators for Refractometry

## Refractive and absorptive properties are inferred by correlating predictions with measurements.

*NASA's Jet Propulsion Laboratory, Pasadena, California*

A method of determining the refractive and absorptive properties of optically transparent materials involves a combination of theoretical and experimental analysis of electromagnetic responses of whispering-gallery-mode (WGM) resonator disks made of those materials. The method was conceived especially for use in studying transparent photorefractive materials, for which purpose this method affords unprecedented levels of sensitivity and accuracy. The method is expected to be particularly useful for measuring temporally varying refractive and absorptive properties of photorefractive materials at infrared wavelengths. Still more particularly, the method is expected to be useful for measuring drifts in these properties that are so slow that, heretofore, the properties were assumed to be constant.

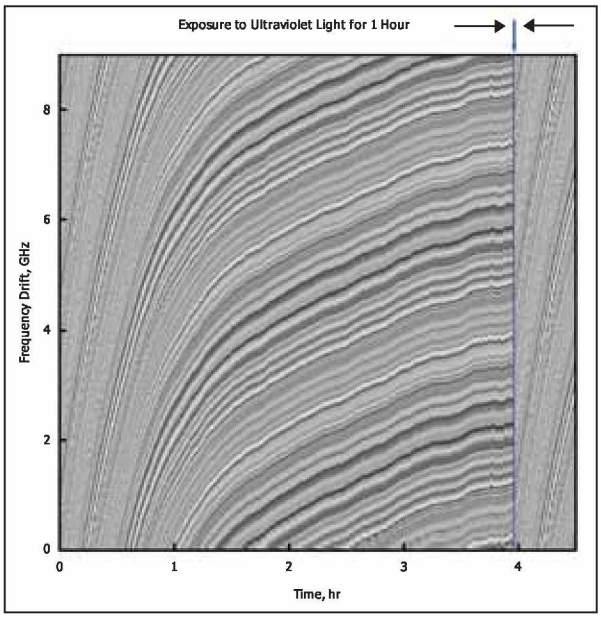


This **Time-vs.-Frequency Plot** shows a saturating drift of the spectrum of a WGM resonator made of a photorefractive material exposed to light. The discontinuity just before the 4-hour mark represents a 1-hour exposure to ultraviolet light, after which the drift of the spectrum recommenced.

The basic idea of the method is to attempt to infer values of the photorefractive properties of a material by seeking to match (1) theoretical predictions of the spectral responses (or selected features thereof) of a WGM of known dimensions made of the material with (2) the actual spectral responses (or selected features thereof). Spectral features that are useful for this purpose include resonance frequencies, free spectral ranges (differences between resonance frequencies of adjacently numbered modes), and resonance quality factors ($Q$ values).

The method has been demonstrated in several experiments, one of which was performed on a WGM resonator made from a disk of $LiNbO_3$ doped with 5 percent of MgO. The free spectral range of the resonator was ≈3.42

GHz at wavelengths in the vicinity of 780 nm, the smallest full width at half maximum of a mode was ≈50 MHz, and the thickness of the resonator in the area of mode localization was 30 μm. In the experiment, laser power of 9 mW was coupled into the resonator with an efficiency of 75 percent, and the laser was scanned over a frequency band 9 GHz wide at a nominal wavelength of ≈780 nm. Resonance frequencies were measured as functions of time during several hours' exposure to the laser light. The results of these measurements, plotted in the figure, show a pronounced collective frequency drift of the resonator modes. The size of the drift has been estimated to correspond to a change of 8.5 $\times 10^{-5}$ in the effective ordinary index of refraction of the resonator material.

*This work was done by Andrey Matsko, Anatoliy Savchenkov, Dmitry Strekalov, Vladimir Iltchenko, and Lute Maleki of Caltech for NASA's Jet Propulsion Laboratory. For more information, contact iaoffice@jpl.nasa.gov. NPO-42694*

# RF Device for Acquiring Images of the Human Body

**This portable, simple system using a ring-shaped antenna array and planar circuit technology can serve as security in airports, mass transit locations, and power plants.**

*NASA's Jet Propulsion Laboratory, Pasadena, California*

A safe, non-invasive method for forming images through clothing of large groups of people, in order to search for concealed weapons either made of metal or not, has been developed. A millimeter wavelength scanner designed in a unique, ring-shaped configuration can obtain a full 360° image of the body with a resolution of less than a millimeter in only a few seconds. Millimeter waves readily penetrate normal clothing, but are highly reflected by the human body and concealed objects. Millimeter wave signals are non-ionizing and are harmless to human tissues when used at low power levels.

The imager (see figure) consists of a thin base that supports a small-diameter vertical post about 7 ft (≈2.13 m) tall. Attached to the post is a square-shaped ring 2 in. (≈5 cm) wide and 3 ft (≈91 cm) on a side. The ring is oriented horizontally, and is supported halfway along one side by a connection to a linear bearing on the vertical post. A planar RF circuit board is mounted to the inside of each side of the ring.

Each circuit board contains an array of 30 receivers, one transmitter, and digitization electronics. Each array element has a printed-circuit patch antenna coupled to a pair of mixers by a 90° coupler. The mixers receive a reference local oscillator signal to a subharmonic of the transmitter frequency. A single local oscillator line feeds all 30 receivers on the board. The resulting MHz IF signals are amplified and carried to the edge of the board where they are demodulated and digitized. The transmitted signal is derived from the local oscillator at a frequency offset determined by a crystal oscillator.

One antenna centrally located on each side of the square ring provides the source illumination power. The total transmitted power is less than 100 mW, resulting in an exposure level that is completely safe to humans. The output signals from all four circuit boards are fed via serial connection to a data processing computer. The computer processes the approximately 1-MB data set into a three-dimensional image in a matter of seconds.

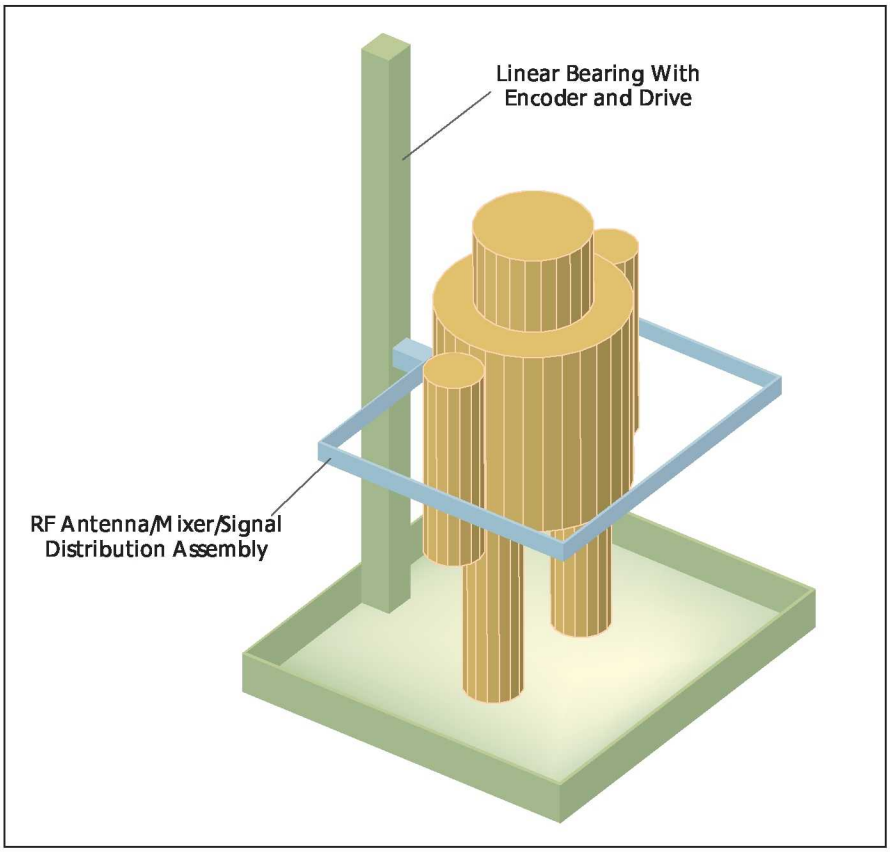


The **RF Imaging Device** can be used in security surveillance of large groups of people to detect concealed metal and non-metal weapons.

The innovation is to configure the receiver array in a ring topology surrounding the scanned object. The ring is then scanned vertically to cover the necessary two-dimensional surface. This fabrication of the ring is made possible by using planar antenna and circuit technology. A planar circuit board serves as a medium for both antennas and signal-processing components. Using this technique, parts counts are kept low, and the cost per element is a small fraction of a waveguide-based system.

*This work was done by Todd C. Gaier and William R. McGrath of Caltech for NASA's Jet Propulsion Laboratory. Further information is contained in a TSP (see page 1).* NPO-42662

# Reactive Collision Avoidance Algorithm

**Algorithm is used for safe operation of autonomous, collaborative, vehicle formations.**

*NASA's Jet Propulsion Laboratory, Pasadena, California*

The reactive collision avoidance (RCA) algorithm allows a spacecraft to find a fuel-optimal trajectory for avoiding an arbitrary number of colliding spacecraft in real time while accounting for acceleration limits. In addition to spacecraft, the technology can be used for vehicles that can accelerate in any direction, such as helicopters and submersibles.

In contrast to existing, passive algorithms that simultaneously design trajectories for a cluster of vehicles working to achieve a common goal, RCA is implemented onboard spacecraft only when an imminent collision is detected, and then plans a collision avoidance maneuver for only that host vehicle, thus preventing a collision in an off-nominal situation for which passive algorithms cannot. An example scenario for such a situation might be when a spacecraft in the cluster is approaching another one, but enters safe mode and begins to drift. Functionally, the RCA detects colliding spacecraft, plans an evasion trajectory by solving the Evasion Trajectory Problem (ETP), and then recovers after the collision is avoided. A direct optimization approach was used to develop the algorithm so it can run in real time.

In this innovation, a parameterized class of avoidance trajectories is specified, and then the optimal trajectory is found by searching over the parameters. The class of trajectories is selected as "bang-off-bang" as motivated by optimal control theory. That is, an avoiding spacecraft first applies full acceleration in a constant direction, then coasts, and finally applies full acceleration to stop.

The parameter optimization problem can be solved offline and stored as a look-up table of values. Using a look-up table allows the algorithm to run in real time. Given a colliding spacecraft, the properties of the collision geometry serve as indices of the look-up table that gives the optimal trajectory. For multiple colliding spacecraft, the set of trajectories that avoid all spacecraft is rapidly searched on-line.

The optimal avoidance trajectory is implemented as a receding-horizon model predictive control law. Therefore, at each time step, the optimal avoidance trajectory is found and the first time step of its acceleration is applied. At the next time step of the control computer, the problem is re-solved and the new first time step is again applied. This continual updating allows the RCA algorithm to adapt to a colliding spacecraft that is making erratic course changes.

*This work was done by Daniel Scharf, Behçet Açikmese, Scott Ploen, and Fred Hadaegh of Caltech for NASA's Jet Propulsion Laboratory. Further information is contained in a TSP (see page 1).*

*The software used in this innovation is available for commercial licensing. Please contact Daniel Broderick of the California Institute of Technology at danielb@caltech.edu. Refer to NPO-44771.*

# Fast Solution in Sparse LDA for Binary Classification

**Special properties of binary classification and greedy algorithms enable speedup.**

*NASA's Jet Propulsion Laboratory, Pasadena, California*

An algorithm that performs sparse linear discriminant analysis (Sparse-LDA) finds near-optimal solutions in far less time than the prior art when specialized to binary classification (of 2 classes). Sparse-LDA is a type of feature- or variable-selection problem with numerous applications in statistics, machine learning, computer vision, computational finance, operations research, and bio-informatics. Because of its combinatorial nature, feature- or variable-selection problems are "NP-hard" or computationally intractable in cases involving more than 30 variables or features. Therefore, one typically seeks approximate solutions by means of greedy search algorithms.

The prior Sparse-LDA algorithm was a greedy algorithm that considered the best variable or feature to add/ delete to/ from its subsets in order to maximally discriminate between multiple classes of data. The present algorithm is designed for the special but prevalent case of "2-class" or binary classification (e.g. 1 vs. 0, functioning vs. malfunctioning, or change versus no change). The present algorithm provides near-optimal solutions on large real-world datasets having hundreds or even thousands of variables or features (e.g. selecting the fewest wavelength bands in a hyperspectral sensor to do terrain classification) and does so in typical computation times of minutes as compared to days or weeks as taken by the prior art.

Sparse LDA requires solving generalized eigenvalue problems for a large number of variable subsets (represented by the submatrices of the input within-class and between-class covariance matrices). In the general (full-rank) case, the amount of computation scales at least cubically with the number of variables and thus the size of the problems that can be solved is limited accordingly. However, in binary classification, the principal eigenvalues can be found using a special analytic formula, without resorting to costly iterative techniques. The present algorithm exploits this analytic form along with the inherent sequential nature of

greedy search itself. Together this enables the use of highly-efficient partitioned-matrix-inverse techniques that result in large speedups of computation in both the forward-selection and backward-elimination stages of greedy algorithms in general.

*This work was done by Baback Moghaddam of Caltech for NASA's Jet Propulsion Laboratory.*

*The software used in this innovation is available for commercial licensing. Please contact Daniel Broderick of the California Institute of Technology at danielb@caltech.edu. Refer to NPO-45333.*

# Modeling Common-Sense Decisions in Artificial Intelligence

## Common sense is implemented partly by feedback from mental to motor dynamics.

*NASA's Jet Propulsion Laboratory, Pasadena, California*

A methodology has been conceived for efficient synthesis of dynamical models that simulate common-sense decision-making processes. This methodology is intended to contribute to the design of artificial-intelligence systems that could imitate human common-sense decision making or assist humans in making correct decisions in unanticipated circumstances. This methodology is a product of continuing research on mathematical models of the behaviors of single- and multi-agent systems known in biology, economics, and sociology, ranging from a single-cell organism at one extreme to the whole of human society at the other extreme. Earlier results of this research were reported in several prior *NASA Tech Briefs* articles, the three most recent and relevant being "Characteristics of Dynamics of Intelligent Systems" (NPO-21037), *NASA Tech Briefs*, Vol. 26, No. 12 (December 2002), page 48; "Self-Supervised Dynamical Systems" (NPO-30634), *NASA Tech Briefs*, Vol. 27, No. 3 (March 2003), page 72; and "Complexity for Survival of Living Systems" (NPO-43302), *NASA Tech Briefs*, Vol. 33, No. 7 (July 2009), page 62.

The methodology involves the concepts reported previously, albeit viewed from a different perspective. One of the main underlying ideas is to extend the application of physical first principles to the behaviors of living systems. Models of motor dynamics are used to simulate the observable behaviors of systems or objects of interest, and models of mental dynamics are used to represent the evolution of the corresponding knowledge bases. For a given system, the knowledge base is modeled in the form of probability distributions and the mental dynamics is represented by models of the evolution of the probability densities or, equivalently, models of flows of information.

Autonomy is imparted to the decision-making process by feedback from mental to motor dynamics. This feedback replaces unavailable external information by information stored in the internal knowledge base. Representation of the dynamical models in a parameterized form reduces the task of common-sense-based decision making to a solution of the following hetero-associated-memory problem: store a set of $m$ predetermined stochastic processes given by their probability distributions in such a way that when presented with an unexpected change in the form of an input out of the set of $M$ inputs, the coupled motor-mental dynamics converges to the corresponding one of the $m$ pre-assigned stochastic process, and a sample of this process represents the decision.

*This work was done by Michail Zak of Caltech for NASA's Jet Propulsion Laboratory. Further information is contained in a TSP (see page 1).* NPO-44114

# Books & Reports

## Graph-Based Path-Planning for Titan Balloons

A document describes a graph-based path-planning algorithm for balloons with vertical control authority and little or no horizontal control authority. The balloons are designed to explore celestial bodies with atmospheres, such as Titan, a moon of Saturn. The algorithm discussed enables the balloon to achieve horizontal motion using the local horizontal winds. The approach is novel because it enables the balloons to use arbitrary wind field models. This is in contrast to prior approaches that used highly simplified wind field models, such as linear, or binary, winds.

This new approach works by discretizing the space in which the balloon operates, and representing the possible states of the balloon as a graph whose arcs represent the time taken to move from one node to another. The approach works with arbitrary wind fields, by looking up the wind strength and direction at every node in the graph from an arbitrary wind model. Having generated the graph, search techniques such as Dijkstra's algorithm are then used to find the set of vertical actuation commands that takes the balloon from the start to the goal in minimum time. In addition, the set of reachable locations on the moon or planet can be determined.

*This work was done by Lars James Blackmore, Nanaz Fathpour, and Alberto Elfes of Caltech for NASA's Jet Propulsion Laboratory. Further information is contained in a TSP (see page 1).* NPO-46607

## Nanolaminate Membranes as Cylindrical Telescope Reflectors

A document discusses a proposal to use axially stretched metal nanolaminate membranes as lightweight parabolic cylindrical reflectors in the Dual Anamorphic Reflector Telescope (DART) — a planned spaceborne telescope in which the cylindrical reflectors would be arranged to obtain a point focus. The discussion brings together a combination of concepts reported separately in several prior *NASA Tech Briefs* articles, the most relevant being "Nanolaminate Mirrors With Integral Figure-Control Actuators" NPO-30221, Vol. 26, No. 5 (May 2002), page 90; and "Reflectors Made From Membranes Stretched Between Beams" NPO-30571, Vol. 33, No. 10 (October 2009), page 11a. The engineering issues receiving the greatest emphasis in the instant document are (1) the change in curvature associated with the Poisson contraction of a stretched nanolaminate reflector membrane and (2) the feasibility of using patches of poly(vinylidene fluoride) on the rear membrane surface as piezoelectric actuators to correct the surface figure for the effect of Poisson contraction and other shape errors.

*This work was done by Jennifer Dooley, Mark Dragovan, Gregory Hickey, and Shyh-Shiu Lih of Caltech for NASA's Jet Propulsion Laboratory. Further information is contained in a TSP (see page 1).*
NPO-40797

## Air-Sea Spray Airborne Radar Profiler Characterizes Energy Fluxes in Hurricanes

A report discusses ASAP (Air-sea Spray Airborne Profiler), a dual-wavelength radar profiler that provides measurement information about the droplet size distribution (DSD) of sea-spray, which can be used to estimate heat and moisture fluxes for hurricane research. Researchers have recently determined that sea spray can have a large effect on the magnitude and distribution of the air-sea energy flux at hurricane-force wind speeds.

To obtain information about the DSD, two parameters of the DSD are required; for example, overall DSD amplitude and DSD mean diameter. This requires two measurements. Two frequencies are used, with a large enough separation that the differential frequency provides size information. One frequency is 94 GHz; the other is 220 GHz. These correspond to the Rayleigh and Mie regions. Above a surface wind speed of 10 m/s, production of sea spray grows exponentially. Both the number of large droplets and the altitude they reach are a function of the surface wind speed.

*This work was done by Stephen L. Durden and D. Esteban-Fernandez of Caltech for NASA's Jet Propulsion Laboratory. Further information is contained in a TSP (see page 1).* NPO-46537

## Large Telescope Segmented Primary Mirror Alignment

A document discusses a broadband (white light) point source, located at the telescope Cassegrain focus, which generates a cone of light limited by the hole in the secondary mirror (SM). It propagates to the aspheric null-mirror, which is optimized to make all the reflected rays to be normal to the primary mirror (PM) upon reflection. PM retro-reflects the rays back through the system for wavefront analysis. The point source and the wavefront analysis subsystems are all located behind the PM. The PM phasing is absolute (white light) and does not involve the SM.

A relatively small, aspheric null-mirror located near the PM center of curvature has been designed to deliver the high level of optical wavefront correction. The phasing of the segments is absolute due to the use of a broadband source. The segmented PM is optically aligned independently and separately from the SM alignment. The separation of the PM segments alignment from the PM to the SM, and other telescope optics alignments, may be a significant advantage, eliminating the errors coupling. The "point source" of this concept is fully cooperative, unlike a star or laser-generated guide-star, providing the necessary brightness for the optimal S/N ratio, the spectral content, and the stable on-axis position. This concept can be implemented in the lab for the PM initial alignment, or made to be a permanent feature of the space-based or ground-based telescope.

*This work was done by Mayer Rud of Caltech for NASA's Jet Propulsion Laboratory. Further information is contained in a TSP (see page 1).* NPO-47032

## Simplified Night Sky Display System

A document describes a simple night sky display system that is portable, lightweight, and includes, at most, four components in its simplest configuration. The total volume of this system is no more than $10^6$ $cm^3$ in a disassembled state, and weighs no more than 20 kilograms. The four basic components are a computer, a projector, a spherical

light-reflecting first surface and mount, and a spherical second surface for display. The computer has temporary or permanent memory that contains at least one signal representing one or more images of a portion of the sky when viewed from an arbitrary position, and at a selected time. The first surface reflector is spherical and receives and reflects the image from the projector onto the second surface, which is shaped like a hemisphere.

This system may be used to simulate selected portions of the night sky, preserving the appearance and kinesthetic sense of the celestial sphere surrounding the Earth or any other point in space. These points will then show motions of planets, stars, galaxies, nebulae, and comets that are visible from that position. The images may be motionless, or move with the passage of time. The array of images presented, and vantage points in space, are limited only by the computer software that is available, or can be developed.

An optional approach is to have the screen (second surface) self-inflate by means of gas within the enclosed volume, and then self-regulate that gas in order to support itself without any other mechanical support.

*This work was done by Timothy P. Castellano of Ames Research Center. Further information is contained in a TSP (see page 1).*

*This invention has been patented by NASA (U.S. Patent No. 7,438,422). Inquiries concerning rights for the commercial use of this invention should be addressed to the Ames Technology Partnerships Division at (650) 604-5761. Refer to ARC-15437-1.*


NASA
National Aeronautics and
Space Administration